nature

https://doi.org/10.1038/s41586-025-09352-w

Accelerated Article Preview

Temperature-Related Hospitalization Burden under Climate Change

Received: 26 March 2025

Accepted: 2 July 2025

Accelerated Article Preview

Cite this article as: Liao, S. et al. Temperature-Related Hospitalization Burden under Climate Change. *Nature* https://doi.org/10.1038/s41586-025-09352-w (2025)

Shujie Liao, Wei Pan, Li Wen, Rongkai chen, Dongyang Pan, Renjie Wang, Cheng Hu, Hongbo Duan, Hong Weng, Chenxiao Tian, Wenxuan Kong, Ruan Jinghan, Yichuan Zhang, Ming Xi, Xianbin Zhang & Xinghuan Wang

Temperature-Related Hospitalization Burden under Climate Change

Shujie Liao[1,6,9†*], Wei Pan[2†*],*Li Wen*[6†], *Rongkai chen*[2†], *Dongyang Pan*[2†], *Renjie Wang*[1†], *Cheng Hu*[3†], *Hongbo Duan*[4†], *Hong Weng*[5, 6†], *Chenxiao Tian*[2], *Wenxuan Kong*[2], *Jinghan Ruan*[7], *Yichuan Zhang*[2], *Ming Xi*[4], *Xianbin Zhang*[8], *Xinghuan Wang*[5, 6*]

[1]Department of Obstetrics and Gynecology, Zhongnan Hospital of Wuhan University, Hubei Province, 430071, China

[2]School of Applied Economics, Renmin University of China, Beijing, 100872, China

[3]Business School, Yangzhou University, Yangzhou, 225127, China

[4]School of Economics & Management, University of Chinese Academy of Sciences, Beijing 100190, China

[5]Department of Urology, Zhongnan Hospital of Wuhan University, Wuhan, 430071, China

[6]Center for Evidence-Based and Translational Medicine, Zhongnan Hospital of Wuhan University, Wuhan, 430071, China

[7]Department of Gynecological Oncology, Tongji Hospital, Tongji Medical College, Huazhong University of Science and Technology, Wuhan, China

[8]Institute of Pharmacy, Shandong University of Traditional Chinese Medicine, Jinan, China

[9]Department of Obstetrics and Gynecology, the Seventh Medical Centre, Chinese PLA General Hospital, Beijing 100700, China

[†]These authors contributed equally: Shujie Liao, Wei Pan, Li Wen, Rongkai Chen, Dongyang Pan, Renjie Wang, Cheng Hu,Hongbo Duan, Hong Weng.

[*]**Corresponding author**

Correspondence to Wei Pan, Shujie Liao, Xinghuan Wang.

Summary

Climate change has significantly increased adverse effects on human health, and economic growth[1–3]. However, few studies have differentiated the impacts of extreme temperatures at the city level, and analysed the future implications for human health under various climate change scenarios.[4–6] Here, data on historical relationship among six kinds of climate-sensitive diseases (CSD) hospitalizations and temperatures across 301 cities (over 90% of all cities) and more than 7,000 hospitals in China are leveraged, and a nonlinear distributed lag model is used. This study projects hospitalization risks associated with extreme temperatures through to the year 2100 and develops the Hospitalization Burden Economic Index to assess the burden under three carbon emission scenarios in cities. Five dimensions including spatial distribution, disease categories, population age groups, future time horizons, and carbon emission development pathways have been evaluated. Historical data specifically indicate more temperature-related risks among the CSDs in northwestern and southwestern China. Notably, gestation-related disease risk is associated with increased vulnerability to extreme heat in specific regions. The projections reveal that, under current thermal conditions with no adaptations, the excess hospitalizations from extreme heat will reach 5.1 million people by 2100 under the high emission scenario.These findings highlight the need for targeted climate change mitigation strategies to reduce uneven climate-related hospitalization risks and economic burdens while accounting for differences in city geography, extreme temperatures, population groups and carbon emission development pathways.

Climate change increasingly endangers human health across generations, both through direct health impacts and through widespread disruptions to environmental and social systems[1–4]. As climate change continued, with extreme temperatures constituting the most widespread and global challenge to public health and health care systems[5,6]. The increasing frequency of extreme temperatures poses intensifying health risks, characterized by thermoregulatory failure leading to organ-specific pathologies through mechanisms such as acute heat-related illnesses, electrolyte imbalances, and the exacerbation of preexisting conditions (e.g., cardiovascular, respiratory, and renal disorders), alongside adverse maternal and neonatal health outcomes as well as climate-sensitive diseasesy[7–9]. Moreover, emerging evidence further identifies pregnancy as a critical vulnerability window, where inflammatory and metabolic stressors increase the risk of preterm birth, gestational diabetes, and related obstetric complications[10]. Concurrently, heat exposure increases the incidence of nephrolithiasis through dehydration, disrupts electrolyte homeostasis, and accelerates both acute kidney injury progression and chronic decline in renal function[7,11,12,]. Temperature-related admissions therefore remain the cardinal sentinel of clinical decompensation[13].

Importantly, the health impacts of extreme temperatures varies across populations and regions due to complex physiological, behavioral, environmental, and socioeconomic interactions. Numerous studies have highlighted greater risks among the elderly[14], newborns[15], and rural populations[16]. Physiological vulnerabilities across age groups differentially exacerbate climate-sensitive health threats. Moreover, inequalities in medical burdens from temperature extremes have been observed across hemispheres[14,17] and ethnic groups[18]. Given the complexity of the issue and the limitations of existing studies, the climate sensitivity of health outcomes to temperature warrants further investigation in broader geographical and demographic contexts.

Cities, as fundamental units of socioeconomic activity and health resource distribution, provide an ideal setting for studying temperature–health dynamics[19]. Urban populations experience relatively uniform climate conditions, lifestyles, and health systems, enabling more precise risk characterization and policy interventions[20]. Furthermore, cities with lower economic development levels may struggle with inadequate medical resources, whereas developed cities face challenges related to chronic disease burdens and mental health issues. Thus, targeted and localized adaptation strategies are necessary to increase resilience to future climate-driven health threats.

While global attention to the health impacts of extreme temperatures has increased[5,7,21], systematic city-level analyses remain rare. China's vast population is distributed across diverse environments, geographical conditions, and demographic backgrounds, leading to heterogeneity in extreme temperature events and associated health risks. This heterogeneity not only poses widespread challenges but also holds great research significance. The cumulative evidence points to systemic vulnerabilities spanning thermoregulatory stress pathways—from cardiovascular decompensation to metabolic dysregulation—with particular severity observed in respiratory, genitourinary, and mental health disorders, while more findings highlight pregnancy as a critical window of climate-sensitive morbidity, as exemplified by heat-related health risks for stroke, stillbirth[9], specific injuries and cardiovascular diseases[22]. Typically regional or monitoring sites

often lack comprehensive analysis at the city level because of data constraints. Moreover, China faces considerable disparities in regional adaptability, medical infrastructure, and socioeconomic conditions. It is necessary to study the impact and preparedness of the health care system in the context of climate change[23,24]. More importantly, previous studies typically emphasize either heat-related or cold-related health impacts independently, often neglecting the differing medical burdens that extreme heat and cold impose on various disease categories. This gap becomes particularly evident under future climate change and socioeconomic uncertainties. Furthermore, studies that consider both temperature extremes simultaneously at the city level remain scarce, especially those that integrate prospective climate warming scenarios.

This study first employs a distributed lag nonlinear model (DLNM) and fixed-effects methods, and uses daily hospitalization data from more than 7,000 hospitals in 301 cities (accounting for more than 90% of all cities) across China between 2021 and 2023 to systematically investigate the historical relationship between temperature fluctuations and hospital admissions (reported as relative risk, RR), differentiating the health impacts of extreme heat and cold, across geographical locations and age groups. Specifically, the analysis included five climate-sensitive disease categories (circulatory, respiratory, endocrine/metabolic, psychiatric, and genitourinary) and one gestation-related category (pregnancy, childbirth, and puerperium-related conditions). This "5+1" classification includes five to the general population and one specific to pregnant women, capturing both general and gestation-related climate-related health risks. Then, future excess hospitalization risks associated with extreme heat and cold temperatures under climate uncertainties (to 2100) are projected by coupling climate change scenarios with shared socioeconomic pathways (SSPs, SSP1-2.6 (low-emission scenario), SSP2-4.5 (medium-emission scenario), and SSP5-8.5 (high-emission scenario)). Finally, this study proposes the Hospitalization Burden Economic Index (HBEI) of excess temperature-related hospitalizations while considering future urban economic development trends. All those works enhance understanding of temperature-sensitive health outcomes, provide evidence to optimize healthcare resources allocation across climates, populations, and disease and further extend these insights into future timeframes and alternative carbon emission scenarios.

Results

Impact of temperature on hospitalization

The historical analysis of temperature-related hospitalization patterns across 295 Chinese cities reveals distinct geographical and demographic variations in health risks, examining spatial distribution, climate-sensitive diseases, and age-specific vulnerability patterns.

Hospitalization patterns demonstrate regional variations in response to extreme heat (Fig. 1a Extended Data Figure 4, and Table S1-4 in SI). Northwest and Southwest China, particularly Gansu (~32°–42°N, 92°–108°E) and Sichuan Provinces (~26°–34°N, 97°–108°E), show higher relative risk (RR) values for heat-related admissions. A 1.5-fold difference in heat effects and 1.2-fold difference in cold effects exists between highest- and lowest-risk regions, with southern and eastern

cities showing enhanced adaptation or reduced inherent risk[25]. Cold exposure analysis (Fig. 1b) revealed elevated RR (>1.300) in northern and western regions, particularly Inner Mongolia (~37°–53°N, 97°–126°E) and Northeast China—areas with lowest annual temperatures and small temperature variability—and in Gansu and Xinjiang (~35°–49°N, 73°–96°E) with low temperatures but greater variability. An intriguing paradox emerges: regions with highest cold sensitivity often coincide with heat risk areas, particularly Northwest and Southwest regions, suggesting compound climate-related health challenges.

Extreme temperature exposure had differential health impacts across disease categories, with respiratory diseases demonstrating pronounced heat-associated risks (RR: 1.056--3.772) (Fig. 1a Extended Data Figure 1, Section 6 in SI). Notably, northern China emerged as the epicenter for heat-related circulatory and respiratory hospitalizations, whereas cold extremes disproportionately affected respiratory health in the northwest. Geospatial analysis revealed that western China is a multirisk hotspot, exhibiting vulnerability to both heat and cold extremes across endocrine, nutritional and metabolic diseases and genitourinary diseases. Geospatial analysis revealed substantial disparities in gestation-related disease (GRD) hospitalization risks across China. As shown in Fig. 1(a6, b6), extreme heat imposed significantly greater burdens (RR: 1.011–1.274) than cold extremes did (RR: 1.002–1.217, RR > 1.1 in only 6 cities), with 151 cities exhibiting heat-related RRs exceeding 1.1. The analysis revealed a novel geographical lens, revealing China's 'GRDs Thermal Risk Demarcation Line' (Extended Data Figure 6, Section 7 in SI), which separates northern heat-vulnerable clusters from southern cold-sensitive zones. This demarcation framework explains the observed hospitalization disparities: North China presented elevated heat-related risks, and South China presented cold-related risks.

Adolescents (0–18 years) and elderly populations showed fluctuating hospital admissions under heat exposure. Surprisingly, adolescents demonstrated high heat sensitivity across multiple urban centers, particularly Beijing, Wuhan (~29°–31°N, 113°–115°E), and Lanzhou (~35°–37°N, 102°–104°E) (Fig.1c). While elderly populations experience greater absolute hospitalizations, adolescents exhibit substantial rate changes in risk per unit temperature increase (Extended Data Figure 5). This heightened adolescent sensitivity may stem from fragile bodies and immature regulatory mechanisms[26]. Analysis of hospital admissions across 21 Chinese provincial capitals revealed minimal sex differences in relative risk (RR) for both extreme heat (95th percentile) and extreme cold (5th percentile), with largely consistent RR values between sexes within cities and higher heat vulnerability in northern cities (Extended Data Fig. 2, Extended Data Fig. 3).

The temperature-health relationship exhibited complex patterns (Fig. 1d, Section 1-5, 8 and Tables S1-1–S1-6 in SI), with strongest negative effects at lowest temperatures and progressively increasing positive coefficients at high temperatures. Temperature variability showed no significant impact ($p = 0.267$), indicating absolute temperature levels drive admissions. Regional analysis demonstrated substantial heterogeneity. The eastern ($p < 0.001$), central ($p = 0.001$), and northwestern ($p < 0.001$) regions show significant increases in hospital admissions during extreme cold events, with the eastern ($p < 0.001$) and central ($p < 0.001$) regions exhibiting nonlinear

relationships. High-temperature impacts are most pronounced in northern ($p = 0.007$) and northeastern ($p = 0.029$) China, with the northern ($p = 0.039$) region showing positive linear effects. Temperature deviation effects are particularly significant in northern ($p < 0.001$), northeastern ($p = 0.018$), and eastern China ($p = 0.011$). The northern region has strong responses to both the temperature range ($p = 0.001$) and standard deviation ($p < 0.001$). Similar patterns appear in the northeastern and eastern regions with varying magnitudes and directions. These findings reveal complex interactions between regional, demographic, and climatic factors, requiring targeted monitoring strategies: northwestern and southwestern regions need attention for both temperature extremes, while central and northeast regions require extreme heat monitoring, and northern regions should prioritize temperature variability assessments

Future frequency of extreme temperatures

Global warming has led to an increase in baseline temperatures, and irreversible temperature changes are occurring across regions under three carbon emission scenarios (Extended Data Figure 7). This study projects the future frequency of temperature extremes, as both extremes could be altered under future climate uncertainties.

Extreme temperature thresholds evolve by scenarios and region across methods (Extended Data Figure 8). Extreme temperature events are becoming increasingly frequent due to future climate change (Fig. 2). Under the current temperature thresholds (T1), extreme weather events across the nation show varying degrees of increase under the three emission scenarios, with the highest increase under the high-emission scenario (projected to exceed 120 days of extreme heat nationwide by 2100), whereas the increase under the low-emission scenario is more moderate, approximately half that under the high-emission scenario. Additionally, the frequency of extreme heat events significantly increases across all three scenarios, particularly in the eastern, central, and southern regions, as well as in the southwest. (Fig. 2a-Fig. 2b). This intensification is especially pronounced under SSP5-8.5. In contrast, the increase in the number of extremely hot days is relatively small in the northern, northeastern, and northwestern regions. Furthermore, the frequency of extremely cold days shows a decreasing trend nationwide, with three emission scenarios remaining at relatively low levels. Notably, when T0 is used as the temperature threshold, the frequency of extreme heat events shows a consistent increasing trend. Moreover, the number of extremely cold days gradually decreased but remained relatively high, especially under SSP1-2.6. Under the T2 threshold, which is calculated iteratively, the frequency of extreme temperature events remains relatively stable, showing minimal changes over time.

The impact of extreme heat shocks varies across regions, particularly under high-emission scenarios, where the increasing frequency of extreme heat events in central, eastern, and southern cities requires urgent attention. Additionally, the disproportionately occurring extreme heat events in the northwest and southwest also warrant vigilance.

Future temperature-hospitalizations risks

This study assesses how future extreme temperature events affect hospitalization risk under different emission scenarios, highlighting health risk disparities across Chinese cities and age groups.The results show that, on the basis of the extreme threshold T1, the risk of excessive hospitalizations associated with extreme heat is projected to progressively increase from 2030 to 2100 across the three scenarios (Fig. 3a), whereas the risk from extreme cold is negligible and shows a declining trend (Fig. 3b). At the national level, the heat hospitalization risk is expected to increase from 2030 (SSP1-2.6: 0.006, SSP2-4.5: 0.028, SSP5-8.5: 0.036) to 2100 (SSP1-2.6: 0.023, SSP2-4.5: 0.108, SSP5-8.5: 0.153). As expected, the risk associated with the high-emission scenario SSP5-8.5 is the highest across all years, increasing by 4.2-fold. Additionally, if the human body gradually adapts to extreme temperatures (T2, Extended Data Figure 10), the associated risks of extreme heat are projected to decrease by 2100, with the risk expected to decline to approximately 0.03.

The excess hospitalization risk varies by location and population (Fig. 3a, Fig. 3b). Under the high-emission scenario, hospitalization risk rises from 0.046 to 0.178 in central, northwestern, southern, and southwestern regions, and from 0.023 to 0.121 in eastern, northern, and northeastern regions. Under the low-emission scenario, the increases are more modest, from 0.006 to 0.024 and 0.006 to 0.020, respectively. Across all the scenarios, the impact remains relatively small in the eastern and northern regions, with overall hospitalization risks nearly half those of the other regions. Moreover, under T2, the hospitalization risk associated with heat and cold decreased, and the increasing trend observed over the years was no longer apparent (Extended Data Figure 10). Excess risks from extreme temperatures vary by age group, with older adults (65+) and teenagers (age<18) being most vulnerable (Fig. 3c，Fig. 3d). In southern, central, and eastern regions, risks are highest for older adults, while in northwestern and southwestern regions, both age groups face similarly high risks. Before 2030–2060, extreme cold has limited impact in most areas, except for slight risks under medium-to-low emission scenarios in northwestern and southwestern China.

Notably, when calculations are performed on the basis of fixed temperature thresholds (T0: 27.5 ℃ for high temperature and 12.5 ℃ for low temperature, Extended Data Figure 9), some intriguing observations emerge. Except for southern China, the risks associated with cold temperatures (below 12.5 ℃) surpass those related to high temperatures (above 27.5 ℃) in all regions (Extended Data Figure 9). In southern regions, however, risks from cold are lower than those from heat, except under the low-emission scenario.

Future heat medical burdens

As Chinese cities face the escalating and varied risks from extreme temperature events, it is imperative to address both current and prospective health care burdens. Based on average city-level hospitalization costs in China in 2022, future excess hospitalization costs due to extreme heat are projected to rise—most sharply under the SSP5-8.5 scenario (Extended Data Figure 11). Nationally, By 2100, excess costs are estimated at approximately 554 million USD under SSP1-2.6, 3780 million USD under SSP2-4.5, and 5190 million USD under SSP5-8.5. Under SSP5-8.5, more than

5.1 million people nationwide are projected to be hospitalized due to heat exposure, with the East, South, and Southwest regions showing relatively higher hospitalization counts among the seven regions (Extended Data Figure 13). These increasing costs show disproportionate trends relative to projected regional GDP growth (Extended Data Figure 11). Moreover, as shown in Extended Data Figure 12, the number of hospitalized individuals due to high temperatures is projected to first increase and then decrease across different regions, with the inflection points varying by region. Under the SSP5-8.5 pathway, the rate of increase is notably faster.

The future heat HBEI is projected to rise progressively, with a complex geographical distribution (Fig. 4a). Hospitalization costs show an inverted U-shaped relationship with economic development, with moderately developed regions—particularly in the southwest—bearing the highest burdens. After 2070, the HBEI under SSP2-4.5 exceeds those under SSP1-2.6 and SSP5-8.5. This is because, although absolute excess hospitalization costs under SSP2-4.5 remain relatively low, GDP growth is also slower, resulting in a higher economic burden index (Extended Data Figure 11). Furthermore, by incorporating city-level healthcare capacity—measured by the number of hospitals—this study examines how economic burdens relate to available medical resources under extreme temperature events (Extended Data Figure 12).

Under different emission scenarios, the future spatial distribution of heat-related HBEI across Chinese cities exhibits significant variation, with clustering patterns in certain typical regions (Fig. 4a). Under the most optimistic scenario (SSP1-2.6), the increase in hospitalization burden is relatively mild (with most cities having an HBEI below 5), except for some cities in the southwestern region around 2070, where the burden warrants attention. In contrast, under the most pessimistic scenario (SSP5-8.5), the spatial pattern of hospitalization burden is more dispersed and shows a gradual, outward spread of increasing burden. Starting from 2030, cities in the southwestern and northwestern regions will face relatively high hospitalization burdens (HBEI large 20 in some cities). Additionally, unlike SSP1-2.6, the northeastern region shows a notably higher burden. The intermediate scenario (SSP2-4.5) reveals a broader and more complex distribution of high-burden areas. By 2030, cities in the northeast and central-southern Yangtze River Basin will begin to face greater medical burdens. By 2070, this trend intensifies, with high-burden zones expanding across the northeast and central regions, leading to greater spatial heterogeneity. By 2100, the situation changes more gradually, suggesting that under this scenario, temperature-related hospitalization burdens will affect a broader range of regions and pose increasing challenges.

Excess hospitalization burdens vary across regions and age groups (Fig. 4b). Under higher emission pathways (SSP2-4.5 and SSP5-8.5), the 65+ population faces an absolutely higher burden across all regions. For the 65+ population, the national average HBEI is projected to rise from 2.4 in 2030 to 12.3 by 2100 under SSP5-8.5. In contrast, HBEI for the 0–18 age group is very low, all at or below 1. In addition, the South and Southwest are projected to face a particularly high healthcare burden in the future—especially in the mid- to long-term—mainly driven by the aging 65+ population, while the burden in the Northeast, North, and East regions remains relatively lower.

Discussion and Implications

Moving beyond traditional single-focus analyses of temperature–health correlations, this research leverages a broader geographical context and hospital admission data to project future hospitalization risks and burdens under different climate change scenarios. Integrating analyses across five dimensions—spatial, disease, age-group, temporal, and emission pathways—it reveals unexpected vulnerability patterns historically and integrates these with future projections. The findings highlight the complex spatial distribution of temperature-related hospitalizations and age-specific vulnerabilities, providing critical insights into climate-health impacts. Economic metrics further quantify societal costs, capturing both health damage and financial losses.

One of the key contributions of this study is the use of unique, high-resolution hospitalization data covering over 7,000 hospitals at the Chinese city level to reveal the spatial distribution patterns of the relationships between various temperature indicators and hospitalization risk. This approach not only more accurately reflects the risks posed by varying temperature conditions across diverse climatic environments but also uncovers the impacts of extreme temperatures from the perspective of the health system process—specifically, at a stage prior to mortality outcomes. Importantly, from the city perspective, heat- and cold-related hospitalization risks exhibit complex spatial distributions, which may be attributed to the combined effects of environmental and climatic characteristics as well as the socioeconomic conditions of cities. Geospatial disparities in GRD heat vulnerability (Fig. 1a6, b6) mirror the "GRD Thermal Risk Demarcation Line" (Extended Data Figure 6), distinguishing heat-vulnerable northern cities from cold-prone southern regions. These patterns likely arise from compounded physiological stresses—elevated cardiovascular load and heat-induced placental dysfunction in third-trimester populations[27]. Although cold impacts are modest, this spatial stratification underscores the need for region-specific, climate-resilient maternal health strategies[10].

Consistent with prior research[19,21], less developed regions bear greater climate-related healthcare burdens than developed areas. Our projections, incorporating future development disparities under SSPs, highlight these differential burdens. Notably, regions with either higher or lower levels of economic development face relatively smaller hospitalization burdens, potentially due to alignment between healthcare demands and resources: wealthier areas have superior infrastructure, while barriers to care access may suppress utilization in poorer regions. Cities with larger populations and higher levels of economic development (such as China's Beijing-Tianjin-Hebei, Yangtze River Delta, and Pearl River Delta city clusters, which collectively account for nearly half of the national GDP and over a quarter of the population) face relatively lower excess hospitalization risks and burdens during extreme temperature periods. This phenomenon may be attributed to the fact that economically developed regions typically possess more abundant resources and well-established infrastructure, thus enabling their ability to effectively mitigate the negative impacts of climate change. In contrast, cities with larger populations but lower economic development (such as China's southwestern region, excluding Chongqing, which accounts for a

relatively small share of the national GDP but over 14–15% of the population and is characterized by mountainous and plateau terrains) experience significantly greater excess hospitalization risks and burdens, further exacerbating the pressure on their health care systems. Also consistent with previous studies, climate risks varied across age groups and diseases, likely due to differing sensitivities and response mechanisms. While elderly populations are traditionally identified as most vulnerable, adolescents (0–18 years) in multiple urban centers also exhibit high heat sensitivity, linked to immature thermoregulatory and metabolic systems increasing risks of dehydration and electrolyte imbalance[11,15,16,49]. Analysis shows individuals aged 65+ currently bear the greatest hospitalization burden, projected to worsen under SSP2-4.5, highlighting how aging exacerbates health care burdens in this scenario.

While the study focuses on China, its methodological framework and findings offer implications for global climate-health research and policy development. The varied temperature–hospitalization relationships across different geographic contexts—from coastal to inland regions and across different latitudinal and longitudinal gradients—provide valuable reference points for establishing global extreme climate health early warning systems tailored to diverse geographical characteristics. The findings demonstrate that regions with similar geographical or climatic conditions worldwide could benefit from comparable adaptation strategies, regardless of national boundaries. This study's economic stratification analysis provides a universal framework for countries across different development stages to anticipate hospitalization burdens under climate change scenarios. Furthermore, the integrated methodological approach combining high-resolution hospitalization data with climate projections establishes a universal framework adaptable to diverse healthcare systems worldwide. This approach advocates for a collaborative global extreme climate health early warning collaboration system that transcends geographical, economic, and political boundaries—where region-specific vulnerability profiles inform resource allocation, whereas standardized metrics enable cross-regional comparison and collaboration.

The findings have several policy implications. Regional heterogeneity highlights diverse climate and economic impacts on health risks, suggesting city-level assessments. Hospitalization rates inform health management, prevention, and early intervention strategies. Prospective results emphasize persistent health impacts due to temperature extremes, underscoring urgent mitigation efforts against global warming. Finally, global inequality highlights the necessity for international collaboration, as regions with limited resources disproportionately suffer from inadequate climate responses, stressing the need for a comprehensive, equitable global climate action framework.

This study uses high-resolution data from 301 Chinese cities to reveal spatially heterogeneous temperature-related hospitalization risks and their future shifts under climate and socioeconomic scenarios, with implications for targeted public health adaptation. These conclusions may interpret with some limitations. The temperature – hospitalization relationships are based on a relatively short observation period (2021 – 2023). While this includes over 1,000 daily data points per site and ensures robust current estimates, it assumes that exposure – response patterns remain stable over time. This approach may overlook future changes in population vulnerability, healthcare systems,

and adaptive capacity, potentially underestimating long-term resilience. Meanwhile, future studies should incorporate dynamic adaptation processes and broader environmental exposures, such as PM_{10}, SO_2, NO_2, and CO, while accounting for possible multicollinearity. In addition, examining finer demographic subgroups could reveal important variations in temperature-related health risks[9].

References

1. Carleton, T. A. & Hsiang, S. M. Social and economic impacts of climate. *Science* **353**, aad9837 (2016).
2. Campbell-Lendrum, D., Neville, T., Schweizer, C. & Neira, M. Climate change and health: three grand challenges. *Nat Med* **29**, 1631–1638 (2023).
3. Wong, C. Climate change is also a health crisis — these 3 graphics explain why. *Nature* **624**, 14–15 (2023).
4. Rising, J., Tedesco, M., Piontek, F. & Stainforth, D. A. The missing risks of climate change. *Nature* **610**, 643–651 (2022).
5. Gasparrini, A. *et al.* Mortality risk attributable to high and low ambient temperature: a multicountry observational study. *The Lancet* **386**, 369–375 (2015).
6. Romanello, M. *et al.* The 2023 report of the Lancet Countdown on health and climate change: the imperative for a health-centred response in a world facing irreversible harms. *The Lancet* **402**, 2346–2394 (2023).
7. Alahmad, B. *et al.* Associations Between Extreme Temperatures and Cardiovascular Cause-Specific Mortality: Results From 27 Countries. *Circulation* **147**, 35–46 (2023).
8. Mahon, M. B. *et al.* A meta-analysis on global change drivers and the risk of infectious disease. *Nature* **629**, 830–836 (2024).
9. Chersich, M. F. *et al.* Associations between high temperatures in pregnancy and risk of preterm birth, low birth weight, and stillbirths: systematic review and meta-analysis. *BMJ* m3811 (2020) doi:10.1136/bmj.m3811.
10. Lakhoo, D. P. *et al.* A systematic review and meta-analysis of heat exposure impacts on maternal, fetal and neonatal health. *Nat Med* (2024) doi:10.1038/s41591-024-03395-8.
11. Hajat, S. *et al.* Ambient heat and acute kidney injury: case-crossover analysis of 1 354 675 automated e-alert episodes linked to high-resolution climate data. *The Lancet Planetary Health* **8**, e156–e162 (2024).
12. Peters, A. & Schneider, A. Cardiovascular risks of climate change. *Nat Rev Cardiol* **18**, 1–2 (2021).
13. Bell, M. L., Gasparrini, A. & Benjamin, G. C. Climate Change, Extreme Heat, and Health. *N Engl J Med* **390**, 1793–1801 (2024).
14. Callaghan, M. *et al.* Machine-learning-based evidence and attribution mapping of 100,000 climate impact studies. *Nat. Clim. Chang.* **11**, 966–972 (2021).
15. Dimitrova, A. *et al.* Temperature-related neonatal deaths attributable to climate change in 29 low- and middle-income countries. *Nat Commun* **15**, 5504 (2024).
16. Zhang, H. *et al.* Unequal urban heat burdens impede climate justice and equity goals. *The Innovation* **4**, 100488 (2023).
17. Zangerl, K. E. *et al.* Child health prioritisation in national adaptation policies on

climate change: a policy document analysis across 160 countries. *The Lancet Child & Adolescent Health* **8**, 532–544 (2024).
18. Deivanayagam, T. A. *et al.* Envisioning environmental equity: climate change, health, and racial justice. *The Lancet* **402**, 64–78 (2023).
19. Grimm, N. B. *et al.* Global Change and the Ecology of Cities. *Science* **319**, 756–760 (2008).
20. Bai, X. *et al.* Six research priorities for cities and climate change. *Nature* **555**, 23–25 (2018).
21. Wu, Y. *et al.* Fluctuating temperature modifies heat-mortality association around the globe. *The Innovation* **3**, 100225 (2022).
22. Yin, P. *et al.* Projection of Mortality Burden Attributable to Nonoptimum Temperature with High Spatial Resolution in China. *Environ. Sci. Technol.* **58**, 6226–6235 (2024).
23. Braithwaite, J. *et al.* Analysing health system capacity and preparedness for climate change. *Nat. Clim. Chang.* **14**, 536–546 (2024).
24. Al-Marwani, S. Climate change impact on the healthcare provided to patients. *Bull Natl Res Cent* **47**, 51 (2023).
25. Kephart, J. L. *et al.* City-level impact of extreme temperatures and mortality in Latin America. *Nat Med* **28**, 1700–1705 (2022).
26. He, Y.-S. *et al.* Time Trends in the Burden of Environmental Heat and Cold Exposure Among Children and Adolescents. *JAMA Pediatr* (2024) doi:10.1001/jamapediatrics.2024.4392.
27. Bonell, A. *et al.* Environmental heat stress on maternal physiology and fetal blood flow in pregnant subsistence farmers in The Gambia, west Africa: an observational cohort study. *The Lancet Planetary Health* **6**, e968–e976 (2022).

Main figure legends

Figure. 1| The impact of temperature on hospital admission. (a, b) Relative risk of extreme heat (a) and cold (b) for hospital admissions at the 95th and 5th percentile temperatures across 295 cities in China over 2021--2023. (1a) and (1b) depict the relative risk of hospitalization associated with extreme heat (a1-a6) and cold (b1-b6) across Chinese cities, stratified by six kinds of climate-sensitive disease categories (circulatory diseases (a1, b1), respiratory diseases (a2, b2), genitourinary diseases (a3, b3), endocrine, nutritional and metabolic diseases (a4, b4), and psychiatric diseases (a5, b5) and gestation-related diseases (GRDs, including pregnancy, childbirth, and puerperium-related conditions) (a6, b6)). The cut-out of islands is the South China Sea Islands. The data for the basis map were sourced from the Standard Map Service Platform (http://bzdt.ch.mnr.gov.cn) supervised by the Ministry of Natural Resources of China. The approval number of basemap is 2023 (2767). The gray areas on the map indicate regions with no data. (c), Age differences in the relative risk of extreme heat versus extreme cold across 21 provincial capital cities in different regions. The risk associated with extreme heat (95th percentile) and extreme cold (5th percentile). (d) Estimated results of the associations between different temperature effects (with 95% CI) and hospital admission. Data are presented as regression coefficients with 95% confidence intervals based on regression analyses with varying sample sizes: North (n=27,894), Northeast (n=36,961), East (n=81,475), South (n=37,552), Central (n=44,943), Southwest (n=40,748), Northwest (n=47,750), and National (n=319,469) observations. (*p<0.1, **p<0.05, ***p<0.01.)

Figure. 2| Future changes in the frequency of extreme heat and cold temperature events. (a) represents the annual frequency of extreme heat events, and (b) represents extreme cold events.

Figure. 3| Excess hospitalization risk in regions related to extreme heat and cold under the T1 threshold calculation for each future year (2030-2100). (a, b) Excess hospitalization risk of future extreme heat and extreme cold events under three emission scenarios. (c, d) Excess hospitalization risk of extreme heat and extreme cold events occurring in the future across the three age groups under the three emission scenarios.

Figure. 4| Future excess heat-related hospitalization medical burden. (a)The hospitalization burden economic index (HBEI) of heat-related hospitalizations in China in the years 2030, 2070 and 2100, reflecting the proportion of excess hospitalization costs due to extreme temperatures relative to the total GDP. The gray areas on the map indicate regions with no data. (b) Heat-attributable HBEI across three age groups and multiple regions.

Methods

Hospitalization data. This study collected hospitalization records covering more than 7,000 hospitals in China from the Clinical Pathway Database (CPD) of the National Health Commission of China. This dataset, which involves standardized clinical pathways, has been required for submission by all hospitals since January 1, 2021. The data indicators included demographic information (sex, age, admission time), hospitalization metrics (actual hospitalization days, medical payment method, health insurance settlement method), and 24 types of cost fields including total hospitalization cost, out-of-pocket hospitalization cost, and medical service fee. In the baseline analysis, this study established a '5+1' climate-sensitive disease framework consisting of: (i) five population-wide disease categories (circulatory diseases [ICD-10: I00-I99], respiratory diseases [J00-J99], endocrine, nutritional and metabolic diseases [E00-E90], psychiatric disorders [F00-F99], and genitourinary diseases [N00-N99]) represented by approximately 78 million data points; and (ii) a special maternal health cohort evaluating gestation-related diseases (ICD-10: O10-O16, O20-O29, O30-O48, and O60-O75). We used the ICD-10 version for standardized diagnostic classification. Age-stratified analyses were conducted across three subgroups (adolescents: 10--18, adults: 19--64, elderly: ⩾65 years), with all subsequent analyses of temperature-hospitalization risk and age-specific effects pertaining to these five major categories of disease unless explicitly stated. Daily averages were processed across 301 prefecture-level cities from January 1, 2021, to December 31, 2023. These 301 cities emerged from comprehensive data quality assessment, wherein all cities with complete hospitalization records were included and deemed adequate for reliable temperature-hospitalization relationship estimation.

Meteorological data. Weather data were obtained from the National Meteorological Information Center of China. The raw data include daily temperature metrics, precipitation, and relative humidity. This study included 699 meteorological stations and adopted the inverse distance weighting method to derive daily weather data for each city. The process involved identifying geometric centers of each prefecture-level city, calculating distances between monitoring stations and city centers, and selecting stations within a 200 km radius. Based on the inverse distance to the city center, weighted averages of daily records were calculated.

Future data. (1) Temperature data utilized for forecasting were sourced from the CMIP6 dataset, representing the sixth iteration of the Coupled Model Intercomparison Project with extensive model participation and comprehensive experimental designs. This dataset covers both historical (1986-2014) and future (2015-2100) periods. Within the CMIP6 dataset, various experimental scenarios are depicted through combinations of shared socioeconomic pathways (SSPs) and representative concentration pathways (RCPs). Four principal scenarios include: (1) SSP1-2.6: low forcing scenario with 2.6 W/m² radiative forcing by 2100; (2) SSP2-4.5: medium forcing scenario reaching 4.5 W/m² by 2100; (3) SSP5-8.5: high forcing scenario leading to 8.5 W/m²

radiative forcing by 2100[28]. (2) **Population projection.** The SSP database aims to document quantitative projections of so-called shared socioeconomic pathways (SSPs) and related integrated assessment scenarios[29]. The gridded population projections for China from 2010–2099 under five SSPs at a resolution of 1 km × 1 km were extracted from the SSP spatial population scenario database. Population projections for each district were computed by aggregating grid cell populations. (3) **GDP projection**. A set of gridded GDP projection data for Chinese cities were obtained, including historical data (represented by 2005) and future projections from 2030-2100 at decadal intervals for all five SSP scenarios[30]. This study utilized the LitPop approach to downscale the 2005 global national GDP and gross regional product (GRP) of over 800 provinces (in 2005 PPP dollars) to a spatial resolution of 30 arc-seconds (approximately 1 km at the equator). The study downscaled national and supranational GDP growth projections under the five SSPs from 2030-2100 to a 1-km grid resolution.

The frequency of future extreme temperature events is calculated. This study considers the temperature-related adaptability calculation, which included three main scenarios. The impacts of future extreme temperature events (2030–2100) were evaluated using threshold values derived from historical temperature data[31,32]. Three representative approaches for defining extreme temperature thresholds were considered: **Threshold 0 (T0):** This approach assumes that temperatures above 27.5 °C are categorized as heat, and those below 12.5 °C are categorized as cold[33,34]. Any temperature outside this range is considered nonoptimal. Under this framework, the total number of days from 2030-2100 with daily mean temperatures exceeding 27.5 °C was counted as heat days, whereas the total number of days with temperatures below 12.5 °C was counted as cold days. **Threshold 1 (T1):** This approach uses the temperature distribution from the last 10-year period (2020–2029) to define thresholds. The 95th percentile of temperatures during this period served as the heat threshold, whereas the 5th percentile served as the cold threshold. These thresholds were fixed and applied consistently across future years. Any day between 2030 and 2100 with temperatures exceeding the heat threshold or falling below the cold threshold was classified as a heat or cold day, respectively. This scenario assumed no temperature adaptation, reflecting how current conditions would respond to future challenges. **Threshold 2 (T2):** In this approach, the thresholds for heat and cold were dynamically updated on the basis of the 10-year period immediately preceding each year of interest. For example, the heat and cold thresholds for 2030 were derived from the 2020–2029 temperature distribution, whereas those for 2050 were derived from the 2040–2049 distribution. A day was classified as a heat or cold day if its temperature exceeded or fell below the corresponding threshold for its preceding 10-year period. Under this scenario, heat and cold thresholds vary with time, representing an adaptive process in response to evolving temperature conditions. Among these, only the T2 scenario is allowed for potential temperature adaptation.

Temperature effect measurements. This study developed a comprehensive three-dimensional framework to investigate the relationship between temperature effects and hospitalization. This framework encompasses temperature frequency effects, temperature intensity

effects, and temperature variability effects, each of which captures distinct aspects of temperature variations through mathematically defined metrics.

This analysis quantified frequency effects through two primary metrics. The first metric, extreme temperature days, measures the occurrence of extreme temperatures:

$$ExtremeDays_{i,t} = \sum_{d=1} D \ \ I\left(Temp_{i,d} > P95\right) + \sum_{d=1} D \ \ I\left(Temp_{i,d} < P5\right)$$

where $I(\cdot)$ is an indicator function and where P95 and P5 represent the 95th and 5th percentile temperature thresholds, respectively. The second metric, consecutive extreme days, measures the maximum duration of consecutive extreme temperatures:

$$ConsecutiveExtremeDays_{i,t} = max\left\{n{:}\cap_{j=0}^{n-1} \ \ I\left(Temp_{i,d} + j > Threshold\right)\right\}$$

Temperature intensity effects are quantified through two measures. The temperature deviation calculates the difference between the daily temperature and the average temperature over a time window:

$$TempDeviation_{i,t} = Temp_{i,d} - 1/w\sum j = t - wt - 1 \ \ Temp_{i,j}$$

The temperature range captures the maximum temperature variation within the time window:

$$TempRangei, t = max_{j\in[t-w,t]}Temp_{i,j} - min_{j\in[t-w,t]}Temp_{i,j}$$

For the temperature variability effects, two statistical measures were employed. The temperature standard deviation is calculated as:

$$TempSD_{i,t} = \sqrt{(1/(w-1)}\sum j = t - wt(Temp_{i,j} - Temp_{i,t})^2$$

The temperature coefficient of variation is expressed as a percentage:

$$TempCV_{i,t} = (TempSD_{i,t}/Temp_{i,t}) \times 100\%$$

In these formulations, *i* denotes the regional index, *t* represents the time index, *w* indicates the time window length, and $Temp_{i,d}$ represents the temperature observed on day *d* before the time *t*. The $Threshold$ can be equal to either $Thresholdhigh$ or $Thresholdlow$, which represent the high and low temperature thresholds, respectively. This comprehensive framework allows us to systematically evaluate how different aspects of temperature variation affect hospitalization.

Distributed Lag Nonlinear Model. This study used a distributed lag nonlinear model (DLNM) model to estimate the impact of temperature exposure. The DLNM assesses the lag effects and nonlinear relationships of environment–exposure–response associations[35]. The hospitalization is not only related to the exposure level on the same day but may also be influenced by exposure over a longer period[36–38].

First stage. Exposure-response and lag-response curves were calculated using time series Poisson regression for specific cities. The basis function response equations are shown below:

$$Log[E(Yi,t)] = \ \alpha \ + \ S(t;\beta) + \ \gamma Dowi,t \ + \ cb(Tt;\theta)$$

where Yi,t denotes the number of hospitalizations in city i at time t, and α is the intercept term. $S(t;\beta)$ is a time-smoothing function with parameter vector β to control for seasonal and long-term trends. $\gamma Dowi,t$ denotes the day-of-week effect. $cb(Tt;\theta)$ is a cross-basis function of temperature, with parameter vector θ. We used 3-fold B-spline with 8 degrees of freedom per year to control for seasonal and long-term trends, with weekly variables for cycle-specific effects. The

exposure-response curve was modeled with quadratic b-spline with interior knots at 10th, 75th, and 90th percentiles, while the lag-response curve used natural cubic b-spline with knots at equally spaced logarithmic values. A 3-day lag period was specified based on established literature. Considering the DLNM model setup, we selected 295 cities with no more than 20% overall missing data and no continuous gaps longer than 30 days to analyze the overall association across five disease categories. For individual diseases and age groups, cities meeting the same criteria were selected accordingly.

Second stage. City-specific results were pooled via multivariate meta-analysis to calculate lowest-risk temperatures and attributable disease burdens. The analysis included environmental and socioeconomic cofactors (annual PM2.5 concentrations, the resident population, education levels, healthcare infrastructure (hospital beds per capita), unemployment rates, and economic development indicators (measured by GDP per capita)) as metapredictors. Monte Carlo simulations calculated empirical confidence intervals.

Econometric model. A two-way fixed effects panel regression model estimated temperature effects on hospitalization:

$$Y_{cd} = \alpha_t + \sum_{h\in\{<-7,\ldots,>28\}} \beta_h cd_h^{MeanTem} + \delta_1 X_{cd} + \sum_{i=1}^{21} \sum_{h\in\{<-7,\ldots,>28\}} \gamma_{hi} c,d - i_h^{MeanTem} + \omega_1 Season_i + \omega_2 Week_i + \varphi_t + \mu_c + \varepsilon_{ct}$$

where Y_{cd} is the average hospitalization case for the c city group at date d, the independent variable is the mean temperature $cd_h^{MeanTem}$, and h denotes the different temperature bins. This analysis divided the distribution of city-level daily temperature, measured in degrees Celsius, into 9 bins: (below −7 °C), [−7 °C -−2 °C), [−2 °C -3 °C), [3 °C - 8 °C), [8 °C -13 °C), [13 °C -18 °C), [18 °C - 23 °C), [23 °C - 28 °C) and [32 °C above). The lowest and highest temperature bins represent extremely cold (below the 5th percentile of the temperature distribution) and extreme heat (above the 95th percentile of the distribution), respectively. The temperature bin [8 °C -13 °C) is considered the optimal temperature and is excluded from the model as a reference group to avoid perfect multicollinearity. This semiparametric approach imposes minimal restrictions and allows for a flexible estimation of the nonlinear effects of temperature on costs. To illustrate, the (below −7 °C) bin equals 1 if the daily temperature falls within this range and equals 0 otherwise, thereby measuring the marginal effects of each temperature bin relative to the optimal temperature. Due to the small number of missing values in the data, we excluded only some of the extreme values in our econometric model to ensure data completeness. The analysis was conducted based on data from 301 cities.

Considering that the short-term impact of temperature on costs is endogenous, this study discussed various specifications to identify its causality as accurately as possible. First, to avoid omitted variable bias, this process sequentially added a series of control variables related to both temperature and medical costs into the model, where X_{cd} represents a set of weather-related variables such as precipitation, relative humidity, and wind speed, along with a set of air pollution-

related variables including PM2.5 and ozone emissions. Second, in some specifications, to account for the serial correlation of temperature and to disentangle the effects of specific dates from the cumulative effects of past temperatures, 21 temperature lags were incorporated into the model. These lags were identified in the same semiparametric manner using temperature bins. Additionally, to better capture cumulative effects, the temperature bin lags were replaced with continuous linear temperature lags. The cumulative effect over the exposure window was assessed by aggregating the lagged coefficients and applying joint significance tests, which allowed for evaluating the overall impact of temperature across multiple lags.

Furthermore, this analysis controlled for time fixed effects and city fixed effects to restrict time trends and adjust for regional differences. Time fixed effects control for confounding factors that vary over time but are constant across cities, such as national policies, economic shocks, or broad seasonal trends. City fixed effects adjust for time-invariant regional differences and baseline climate characteristics, thus ensuring that the model captures within-city variations in temperature rather than between-city differences. Since time fixed effects may not fully account for short-term fluctuations such as seasonal variations or weekly cyclical patterns, this study also included seasonal and weekday dummy variables. These variables address more granular fluctuations that time fixed effects might miss, providing a more robust model.

The Hospitalization Burden Economic Index (HBEI) is calculated as the ratio of hospitalization costs attributed to extreme temperatures in a specific region to the adjusted GDP of the region (GDP minus hospitalization costs). This study consider the proportion of an individual's medical expenses relative to their remaining disposable income as a measure of financial burden[39–41].The hospitalization costs are calculated by multiplying the disease excess hospitalizations due to heat and cold by the average hospitalization cost. The average hospitalization cost is calculated on the basis of the national mean of inpatient expenses due to illness from 2021-- 2023 and is determined separately for each subgroup. **City level:** The average hospitalization cost for each of the five major disease categories, calculated across all individuals within the observation period. **Age group level:** The average cost for each age group was calculated on the basis of city-specific hospitalization data for different age groups. The GDP levels of each region are based on the total GDP values obtained through projections. The ratio is then multiplied by 10,000 to standardize the values for easier interpretation, as regional total GDP is typically on the scale of trillions. Under this calculation, the HBEI represents the contribution of hospitalization costs due to extreme heat or cold to the total city GDP. Generally, a lower HBEI during extreme events indicates a lower resilience of the city or population to such events, whereas a higher HBEI suggests greater adaptive capacity or emergency response capability.

In addition, this study acknowledge that the hospitalization cost estimates in this study are based on current expenditure levels, whereas future hospitalization costs are influenced by a range of additional factors, such as advances in medical technology, policy and regulatory changes, and climate change itself[42,43]. Therefore, alongside projecting future hospitalization costs associated

with extreme heat, this analysis also calculated 95% confidence intervals for hospitalization costs related to five major climate-sensitive disease categories under three carbon emission pathways, accounting for future climate change scenarios. This study clarified that the calculations do not incorporate assumptions regarding technological progress or other adaptive measures. Furthermore, in HBEI calculation, this study replaced the projected excess hospitalization costs due to heat with the projected excess number of hospitalizations to assess the robustness of the HBEI. This approach acknowledges that, beyond the financial burden, a sudden surge in patient numbers within a short timeframe can severely affect hospital services, compromise urban public health systems, and challenge the overall resilience of cities.

Forecasting methods. The specific methods for forecasting changes in medical burden due to extreme temperatures involve the following three steps:

First, a DLNM was applied to elucidate the exposure–response relationship $f(T, H)$between daily average temperatures in domestic prefecture-level cities and the corresponding number of hospitalizations. Here, the abovementioned DLNM is fully applied to the existing data for city-specific training, and parameter estimates are generated as outputs.

Second, the temperature was projected via global climate models (GCMs). The temperature projections are derived from twelve global climate models. The China Regional Surface Meteorological Element Driving Dataset (CMDF) grid precipitation and temperature data are used as observational references. The temperature data from these models are subjected to bias correction through the equidistant cumulative distribution function method following bilinear interpolation to a 0.25° grid, yielding daily average temperature data for each city under various SSP scenarios. This study used 12 GCM models to calculate the projected daily mean temperature for each city from 2030-- 2100. The GCM models applied include *KACE-1-0-G, NorESM2-MM,NorESM2-LM,INM-CM5-0,INM-CM4-0,TaiESM1,MRI-ESM2-0,MPI-ESM1-2-HR,IPSL-CM6A-LR,GFDL-CM4,CanESM5,FGOALS-g3.* This multimodel approach helps mitigate the instability associated with relying on a single GCM and enhances the robustness of the temperature projections.

Finally, health indicator estimation was performed by incorporating the improved temperature data into the initial exposure–response model to estimate the impact of temperature changes on the number of relevant hospitalizations under different SSP scenarios. On the basis of the DLNM temperature–mortality relationship, this study calculated the daily historical and future numbers of temperature–attributable hospitalizations H_{temp} on any day with daily mean temperatures above T_{mm} as follows:

$$H_{temp} = H(1 - e^{-\left(f^*(proj_*^T;\ b_*^\theta)\right)-\left(f^*(T_{mm};\ b_*^\theta)\right)})$$

where f^* denotes the overall cumulative temperature–hospitalization association derived from the bidimensional term in the adjusted DLNM estimation, where $proj_*^T$ represents the projected temperature series, *H* represents the total number of hospitalizations for a given area, either overall or disaggregated by population group and disease. The number of hospitalizations attributable to

temperatures was calculated by summing subsets of days with temperatures above T_{mm}. This calculation separated components due to heat and cold by summing the subsets corresponding to days with temperatures higher or lower than T_{mm}.

Decadal temperature-related excess hospitalization was separately estimated for each city and for combinations of SSPs and GCMs. Subsequently, attributable fractions as GCM-ensemble means according to region, hospitalizations and the SSPs were further calculated using the corresponding total number of hospitalizations as the denominator.

Uncertainty analysis. The uncertainties in projecting future temperature-related hospitalizations primarily stem from the temperature–hospitalization relationship, the variation in temperature projections across different GCMs, and population projections. The uncertainty in projected populations was addressed using three SSP scenarios, which encompass high, medium, and low emission pathways.

Vulnerable subgroups and population aging. To identify future high- and low-temperature–susceptible subgroups, this study conducted the above analyses by disease, age, and sex. Based on the temperature–hospitalization relationships within each subgroup, it projected the attributable proportions and numbers of hospitalizations under future high- and low-temperature conditions. Specifically, future estimates of hospitalizations for various population groups (0–18, 19–64, and 65+; male and female) and for different diseases rely on linear projections derived from the 2022 city-level hospitalization data collected by the National Health Commission, along with nationwide hospitalization rates for each demographic and disease group and future population projections under three SSP scenarios.

Data availability

The national hospitalization data are confidential and obtained from the National Health Commission of China. To enhance transparency while adhering to data protection policies, we have publicly released **city-level daily hospitalization counts** and **average hospitalization costs**, with all city names anonymized and replaced by coded identifiers. All shared data are accessible via [https://zenodo.org/records/15752585]. Meteorological data were obtained from the ECMWF ERA5 dataset (https://cds.climate.copernicus.eu/cdsapp#!/dataset/sis-agrometeorological-indicators?tab=overview). The temperature data used for forecasting were sourced from the CMIP6 dataset (https://cds.climate.copernicus.eu/datasets/projections-cmip6?tab=overview).The population projection data were derived from publicly available data in a research paper (https://cloud.tsinghua.edu.cn/f/d593f46793fb4145b8b9/?dl=1). The GDP projection data were obtained from publicly available data in a research paper (https://zenodo.org/records/5880037). Other economic and geographic information related to Chinese cities was sourced from the National Bureau of Statistics of China (https://www.stats.gov.cn/sj/ndsj/).

Code availability

This study conducts a historical analysis of the relationship between temperature and hospitalizations via the DLNM approach. It further implements extreme weather projections based on three different temperature threshold calculation methods to assess future climate impacts. These analyses project health risks under extreme heat and cold conditions for each city over 2030-2100. Finally, it estimates the excess medical burden by integrating the projected hospitalization risks with the future population and GDP projections, providing a comprehensive assessment of the potential healthcare challenges associated with climate change. All of the codes can be accessed at https://zenodo.org/records/15752585.

Contributions

X.H.W., W.P., S.J.L. designed and supervised the study. L.W. and R.K.C. conducted the study, collected the data, analyzed the results and drafted the paper. D.Y.P., R.J.W., C.H., J.H.R., H.W. provided calculations and writing related to economics model, disease, and public health. C.X.T. collected and processed the meteorological and temperature data and drafted the paper. Y.C.Z. collected and processed the population data and other data collected. D.Y.P., X.M., X.Z. and H.B.D. provided guidance on the analysis and assessment of health and medical burden. R.K.C., L.W., and W.X.K. guided the uncertainty analysis and validation.

References

28. O'Neill, B. C. *et al.* The Scenario Model Intercomparison Project (ScenarioMIP) for CMIP6. *Geosci. Model Dev.* **9**, 3461–3482 (2016).
29. Zhang, S. *et al.* City-level population projection for China under different pathways from 2010 to 2100. *Sci Data* **10**, 809 (2023).
30. Wang, T. & Sun, F. Global gridded GDP data set consistent with the shared socioeconomic pathways. *Sci Data* **9**, 221 (2022).
31. Guo, Y. *et al.* Global Variation in the Effects of Ambient Temperature on Mortality: A Systematic Evaluation. *Epidemiology* **25**, 781–789 (2014).
32. Zhang, X. *et al.* Indices for monitoring changes in extremes based on daily temperature and precipitation data. *WIREs Climate Change* **2**, 851–870 (2011).
33. Colelli, F. P., Emmerling, J., Marangoni, G., Mistry, M. N. & De Cian, E. Increased energy use for adaptation significantly impacts mitigation pathways. *Nat Commun* **13**, 4964 (2022).
34. De Cian, E. & Sue Wing, I. Global Energy Consumption in a Warming Climate. *Environ Resource Econ* **72**, 365–410 (2019).
35. Zhang, S. *et al.* Heat and cause-specific cardiopulmonary mortality in Germany: a case-crossover study using small-area assessment. *The Lancet Regional Health - Europe* **46**, 101049 (2024).

36. García-León, D. *et al.* Temperature-related mortality burden and projected change in 1368 European regions: a modelling study. *The Lancet Public Health* **9**, e644–e653 (2024).
37. Liu, C. *et al.* Ambient Particulate Air Pollution and Daily Mortality in 652 Cities. *N Engl J Med* **381**, 705–715 (2019).
38. Chen, G. *et al.* All-cause, cardiovascular, and respiratory mortality and wildfire-related ozone: a multicountry two-stage time series analysis. *The Lancet Planetary Health* **8**, e452–e462 (2024).
39. OECD. Framework for Statistics on the Distribution of Household Income, Consumption and Wealth. *Paris: OECD Publishing.* (2013).
40. McIntyre, D., Thiede, M., Dahlgren, G. & Whitehead, M. What are the economic consequences for households of illness and of paying for health care in low- and middle-income country contexts? *Social Science & Medicine* **62**, 858–865 (2006).
41. Xu, K. *et al.* Protecting Households From Catastrophic Health Spending. *Health Affairs* **26**, 972–983 (2007).
42. Watts, N. *et al.* Health and climate change: policy responses to protect public health. *The Lancet* **386**, 1861–1914 (2015).
43. Kinney, P. L. Climate Change, Air Quality, and Human Health. *American Journal of Preventive Medicine* **35**, 459–467 (2008).

Corresponding author

Correspondence to Wei Pan, Shujie Liao, Xinghuan Wang.

Competing interest statement

The authors declare no competing interests

Ethical approval statement

This study was approved by Medical Ethics Committee, Zhongnan Hospital of Wuhan University (Approval No. 2024297K, Approval Date: 10, December 2024). All procedures adhered to the ethical standards of this committee and applicable national regulations. The revised manuscript reflects this addition, and the ethics documentation remains available for editorial verification upon request.

Acknowledgements

This research was funded by National Natural Science Foundation of China (NSFC) (Grant no. 72474218; 82341120; 82372354; 72202229; 72325008).

Extended Data Figure legends

Extended Data Figure 1. Causes of differences in the relative risk of extreme heat versus extreme cold in cities in different regions. RR of hospital admissions at the 95th (a) and 5th (b) percentile temperatures for five different disease categories—circulatory, respiratory, genitourinary, endocrine, nutritional and metabolic diseases, and psychiatric diseases—across 21 provincial capital cities in China. The top panel displays the RR for extremely high temperatures (95th percentile), whereas the bottom panel shows the RR for extremely low temperatures (5th percentile). Each point represents the estimated RR for a specific disease category, providing a detailed analysis of how extreme temperatures impact hospital admissions for different health conditions.

Extended Data Figure 2. Sex differences in the relative risk of extreme heat versus extreme cold in cities in different regions. The vertical axis of the figure is RR. The figure presents RRs of hospital admissions at the 95th (a) and 5th (b) percentile temperatures for males and females across 21 provincial capital cities selected from the seven geographic regions in China. Each point represents the estimated RR for males and females, allowing for comparisons between sexes and across different cities.

Extended Data Figure 3. Relative risk of hospital admission for males under extreme heat (a) versus extreme cold (b) and females under extreme heat (c) versus extreme cold (d) in Chinese cities.

Extended Data Figure 4. Relative risk of hospitalization at the 95th percentile (high) and 5th percentile (low) temperatures for each city grouped by region.

Extended Data Figure 5. Hospital admissions across temperature percentiles by age group. The x–axis represents temperature percentiles, with lower percentiles (colder temperatures) on the left and higher percentiles (warmer temperatures) on the right. The y–axis shows the number of hospital admissions, with different age groups distinguished by color.

Extended Data Figure 6. Impact of temperature on hospital admission for gestation–related disease (GRDs). Geographic distribution of extreme temperature–associated hospitalization risks for GRDs across Chinese cities, showing extreme heat (a) and cold (b) patterns. (a) GRDs thermal risk demarcation line for extreme heat , where cities north of this threshold (red dashed line) (~31°N) present elevated relative risks for GRDs hospitalizations. (b) GRDs thermal risk demarcation line of extreme cold , with cities south of this threshold (blue dashed line) (~39°N) demonstrating increased cold–associated risk.

Extended Data Figure 7. Future temperature change trends across different regions under three emission scenarios.

Extended Data Figure 8. Future temperature thresholds across different regions are calculated via three evaluation methods for extreme temperatures, a for heat and b for cold.

Extended Data Figure 9. Future excess hospitalization risks attributed to high (a) and low (b) temperatures. (T0, above 27.5°C and below 12.5°C).

Extended Data Figure 10. Future excess hospitalization risks attributed to high (a) and low (b) temperatures. (T2, temperature thresholds change annually, assuming a trend of temperature adaptation).

Extended Data Figure 11. Future regional excess hospitalization costs and GDP (Unit: RMB (billion) , **T1, no adaptation). a** represents the excess heat–related costs, and **b** represents the GDP under different carbon emission scenarios.

Extended Data Figure 12. Relationship between HBEI and hospital availability under extreme heat across three emission scenarios. Number of Hospitals represents the total number of hospitals in each city, while Number of Class III Hospitals refers to tertiary hospitals, which provide more comprehensive and higher-quality medical care.

Extended Data Figure 13. Excess hospitalizations attributable to extremely high and low temperatures across different regions.

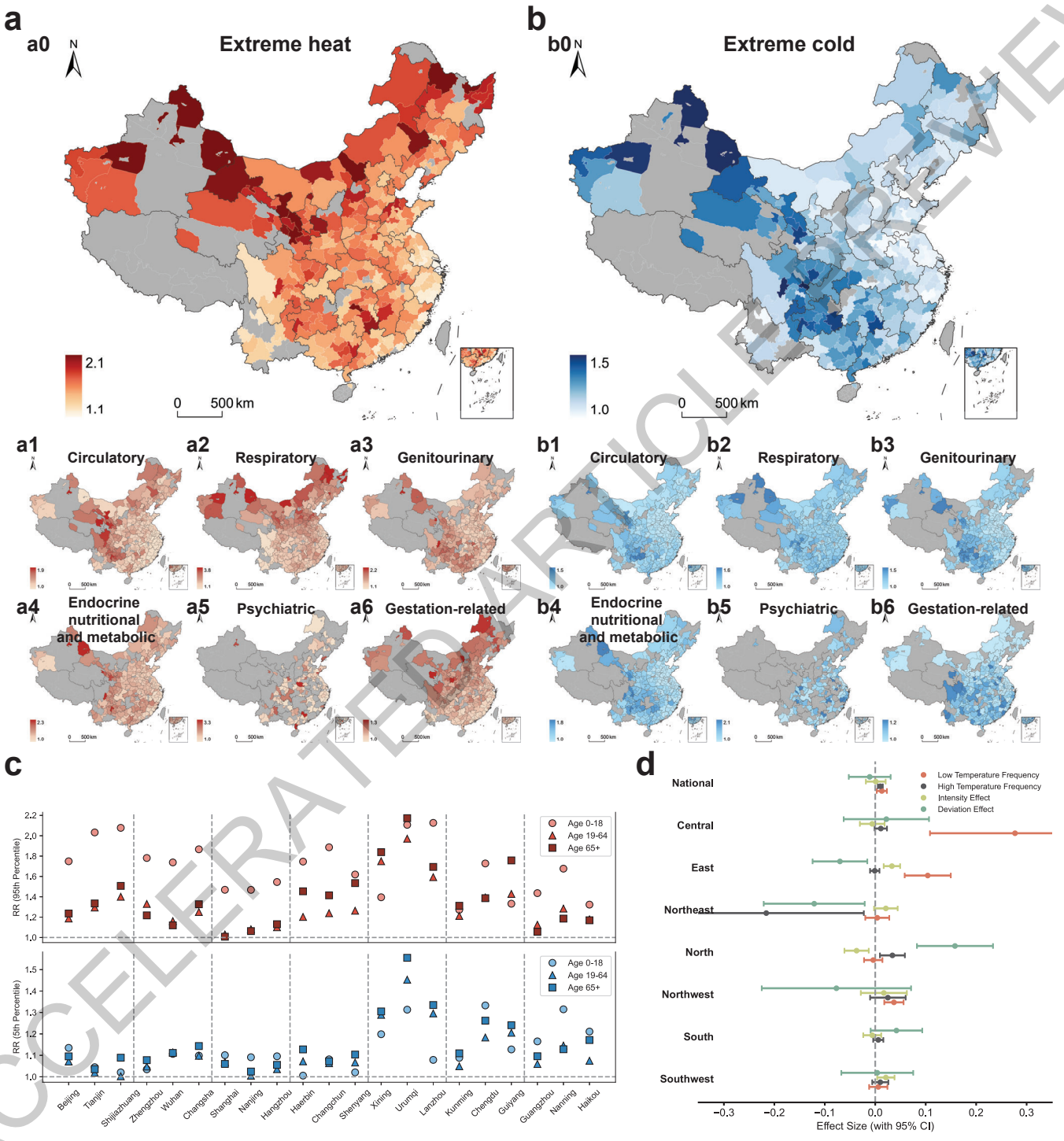

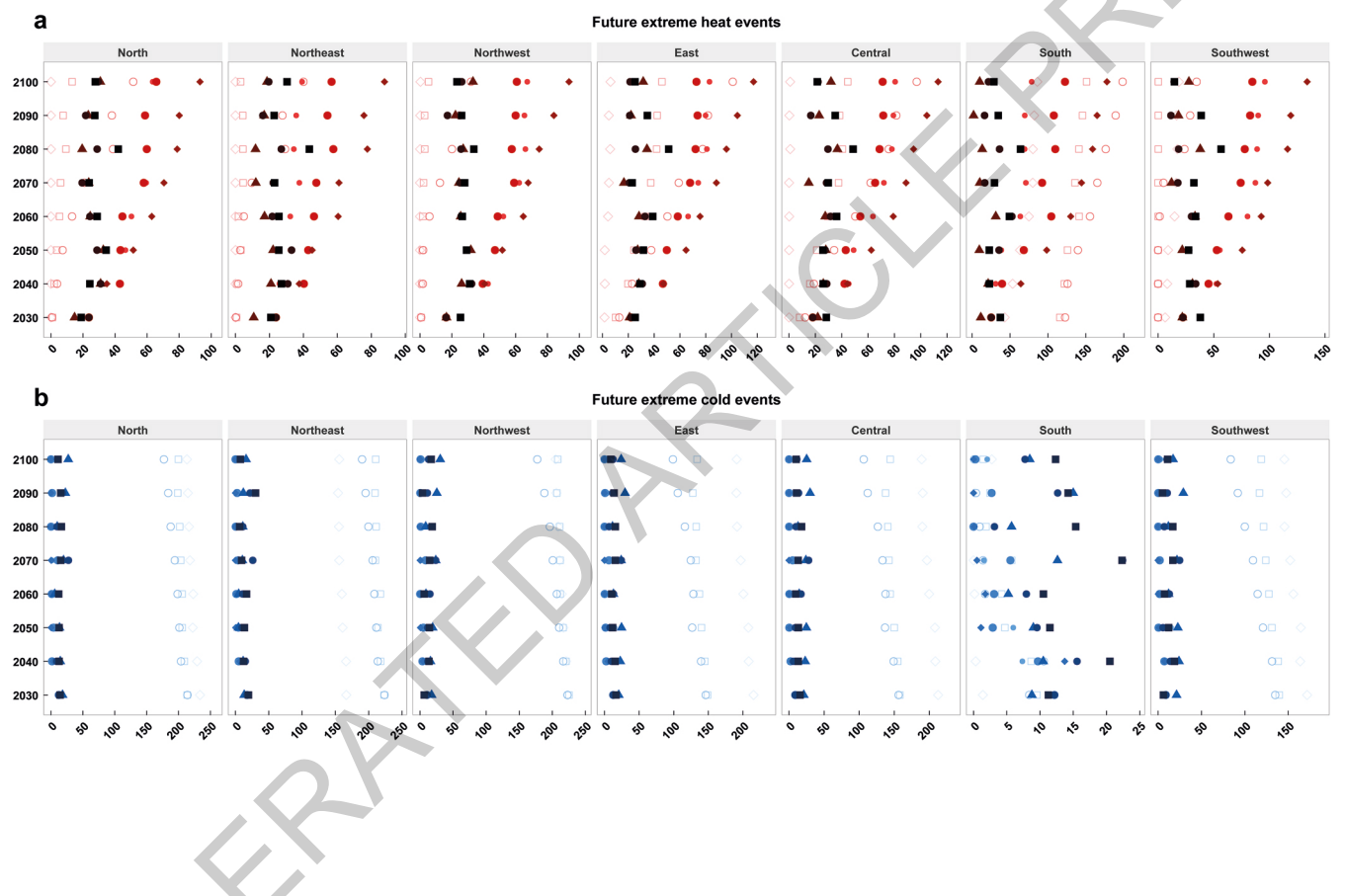

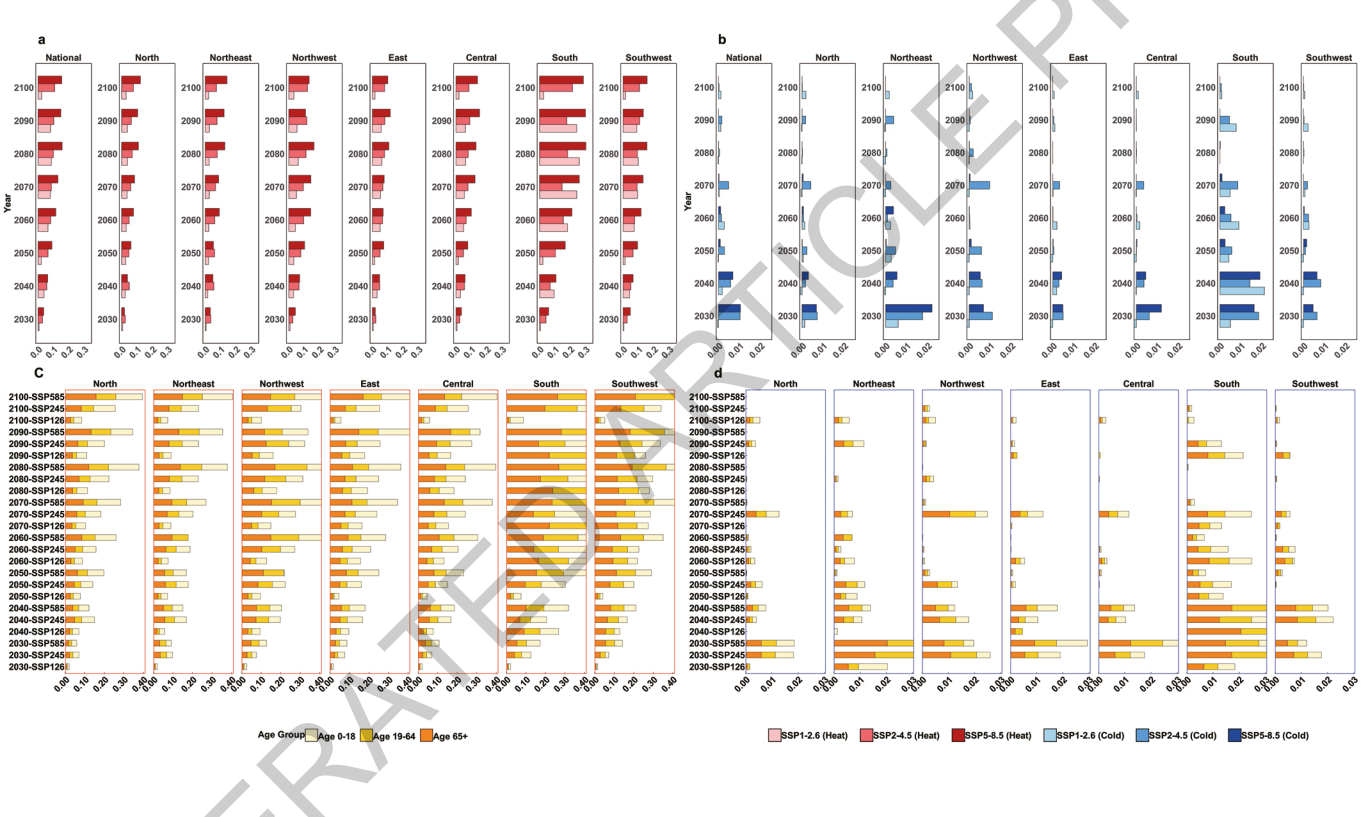
a
National
North
Northeast
Northwest
East
Central
South
Southwest
Year
2100
2090
2080
2070
2060
2050
2040
2030
0.0
0.1
0.2
0.3
b
0.00
0.01
0.02
c
North
Northeast
Northwest
East
Central
South
Southwest
2100-SSP585
2100-SSP245
2100-SSP126
2090-SSP585
2090-SSP245
2090-SSP126
2080-SSP585
2080-SSP245
2080-SSP126
2070-SSP585
2070-SSP245
2070-SSP126
2060-SSP585
2060-SSP245
2060-SSP126
2050-SSP585
2050-SSP245
2050-SSP126
2040-SSP585
2040-SSP245
2040-SSP126
2030-SSP585
2030-SSP245
2030-SSP126
0.00
0.10
0.20
0.30
0.40
Age Group
Age 0-18
Age 19-64
Age 65+
d
0.00
0.01
0.02
0.03
SSP1-2.6 (Heat)
SSP2-4.5 (Heat)
SSP5-8.5 (Heat)
SSP1-2.6 (Cold)
SSP2-4.5 (Cold)
SSP5-8.5 (Cold)

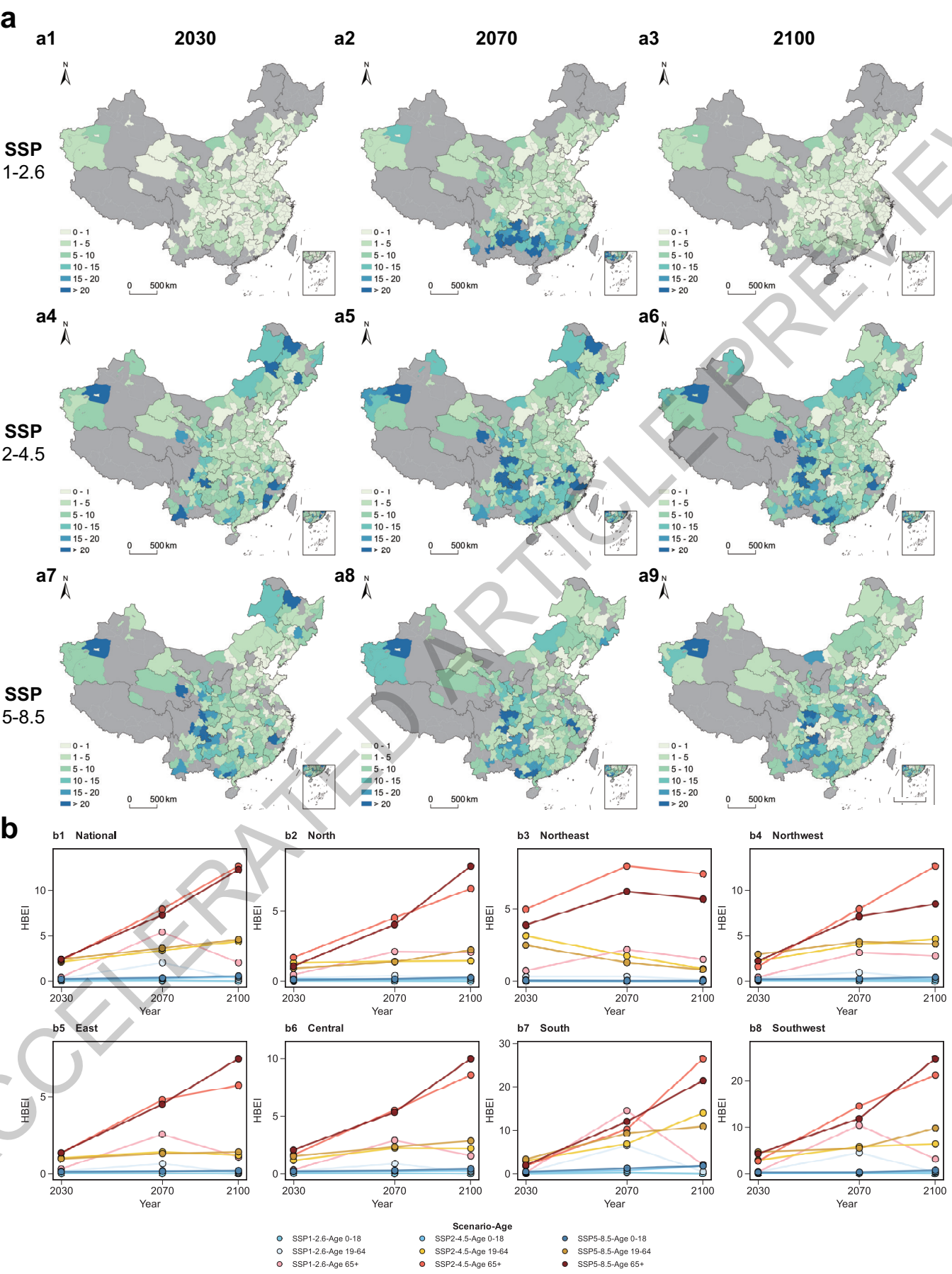

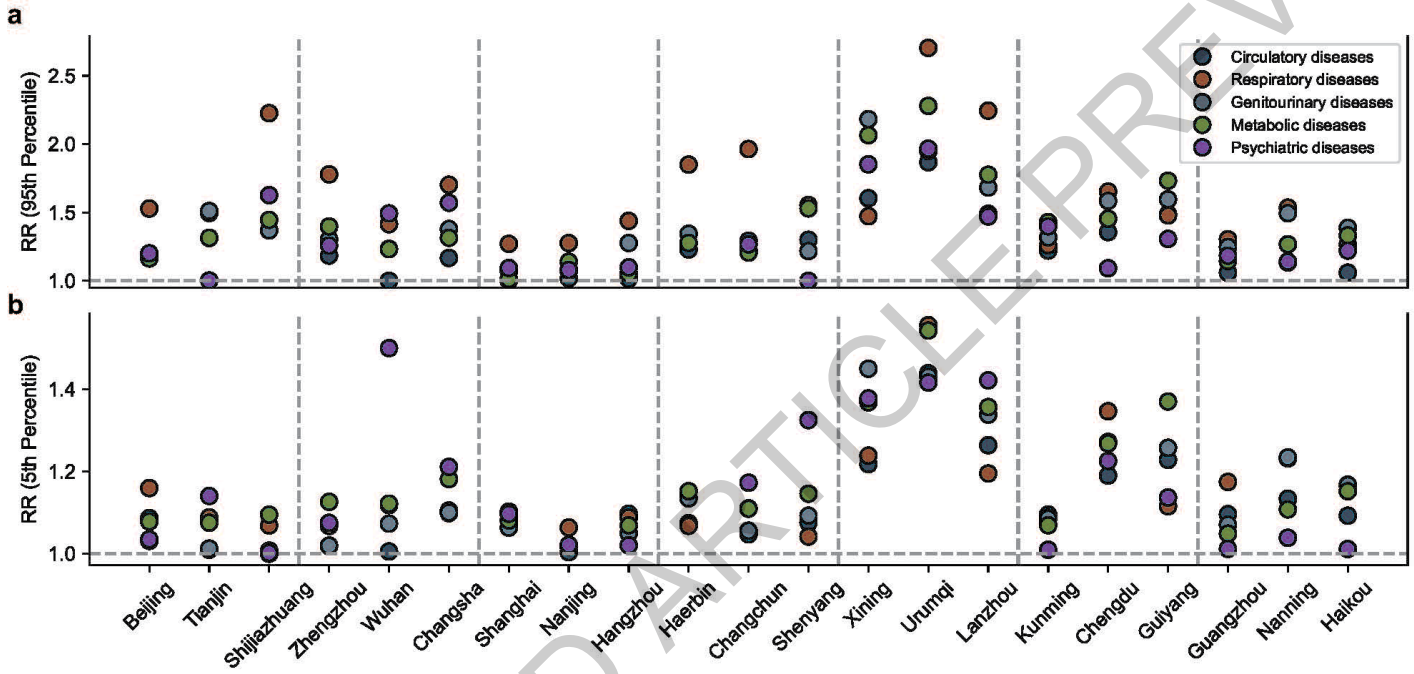

Extended Data Fig. 1

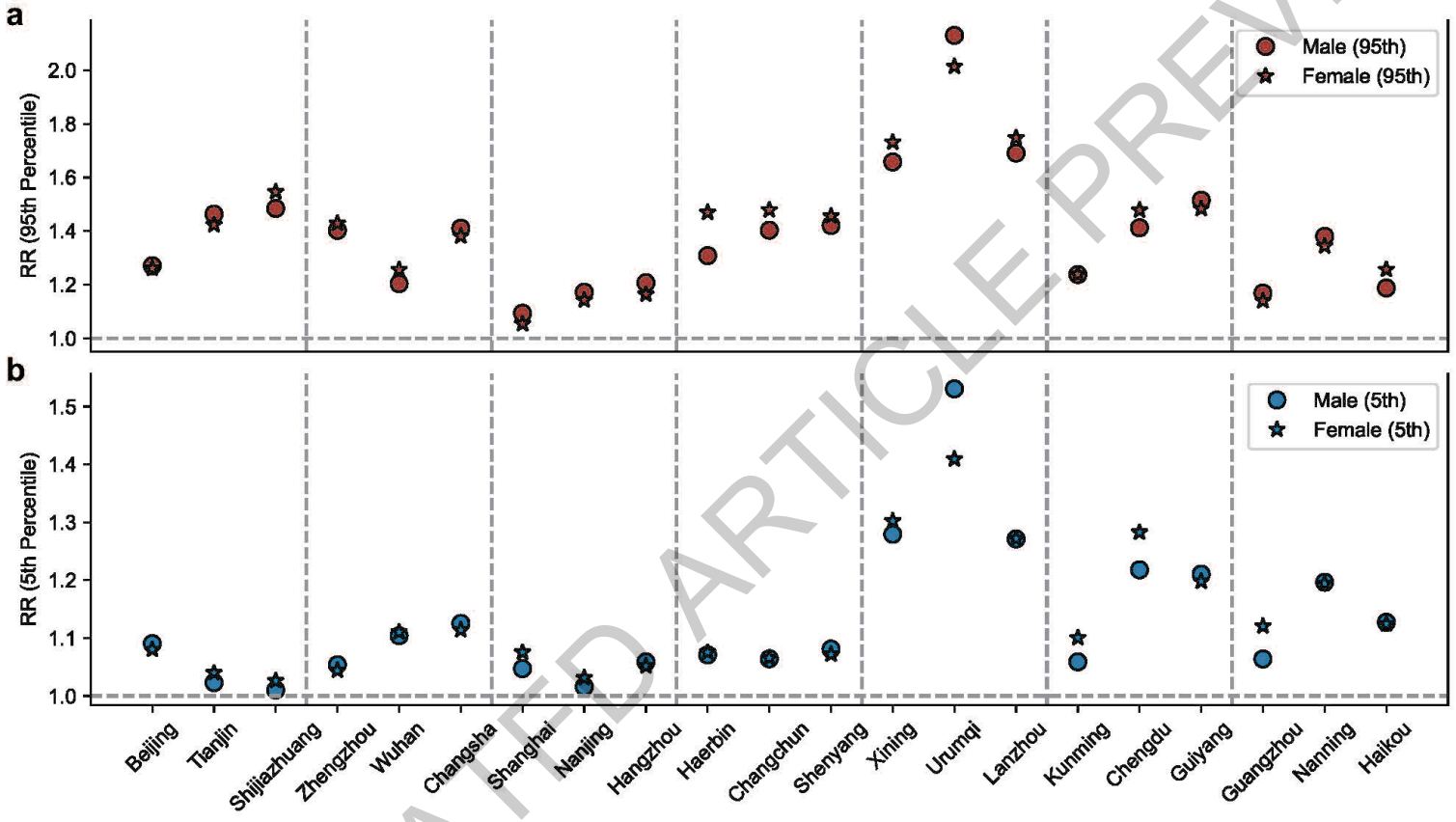

Extended Data Fig. 2

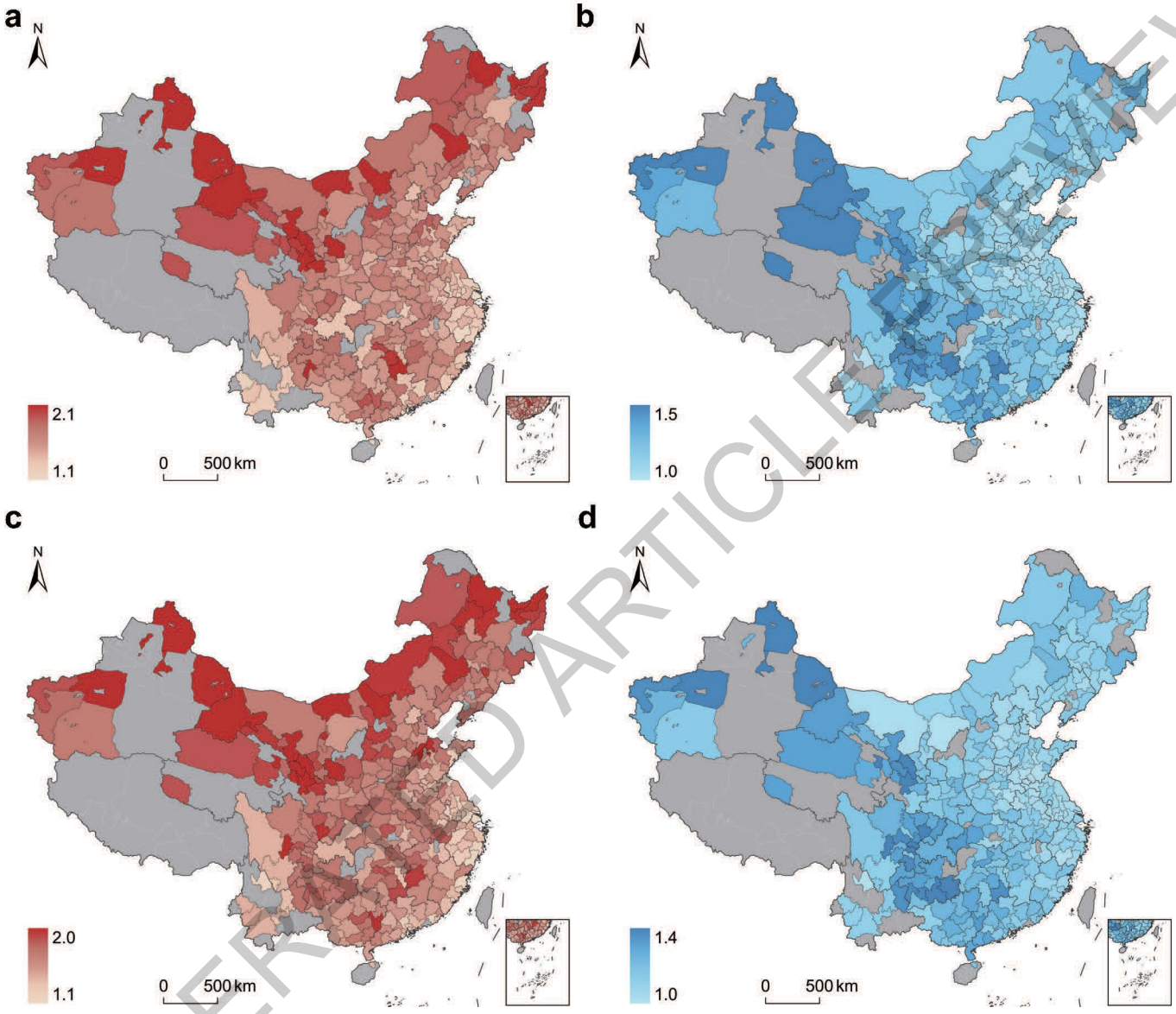

Extended Data Fig. 3

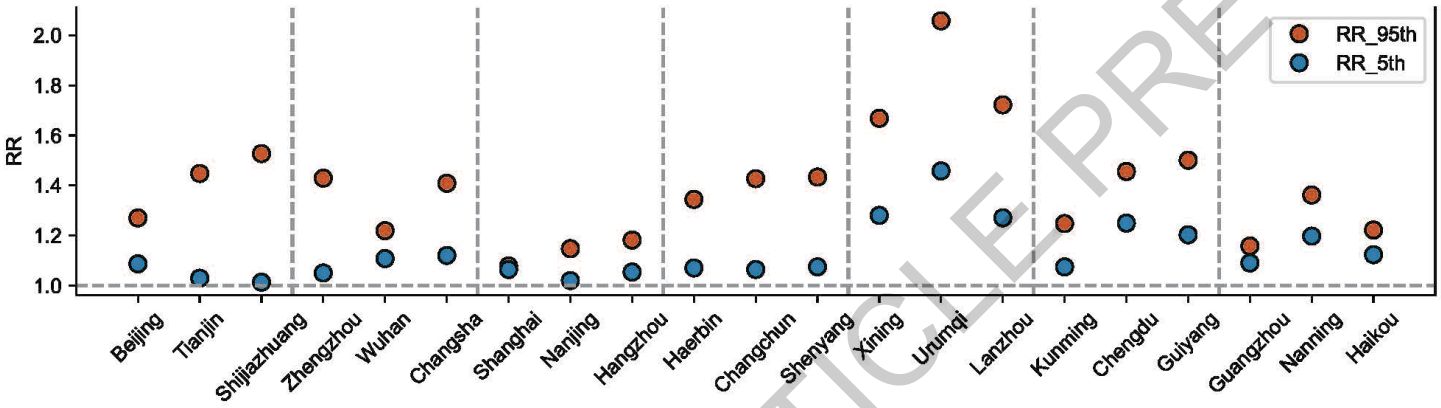

Extended Data Fig. 4

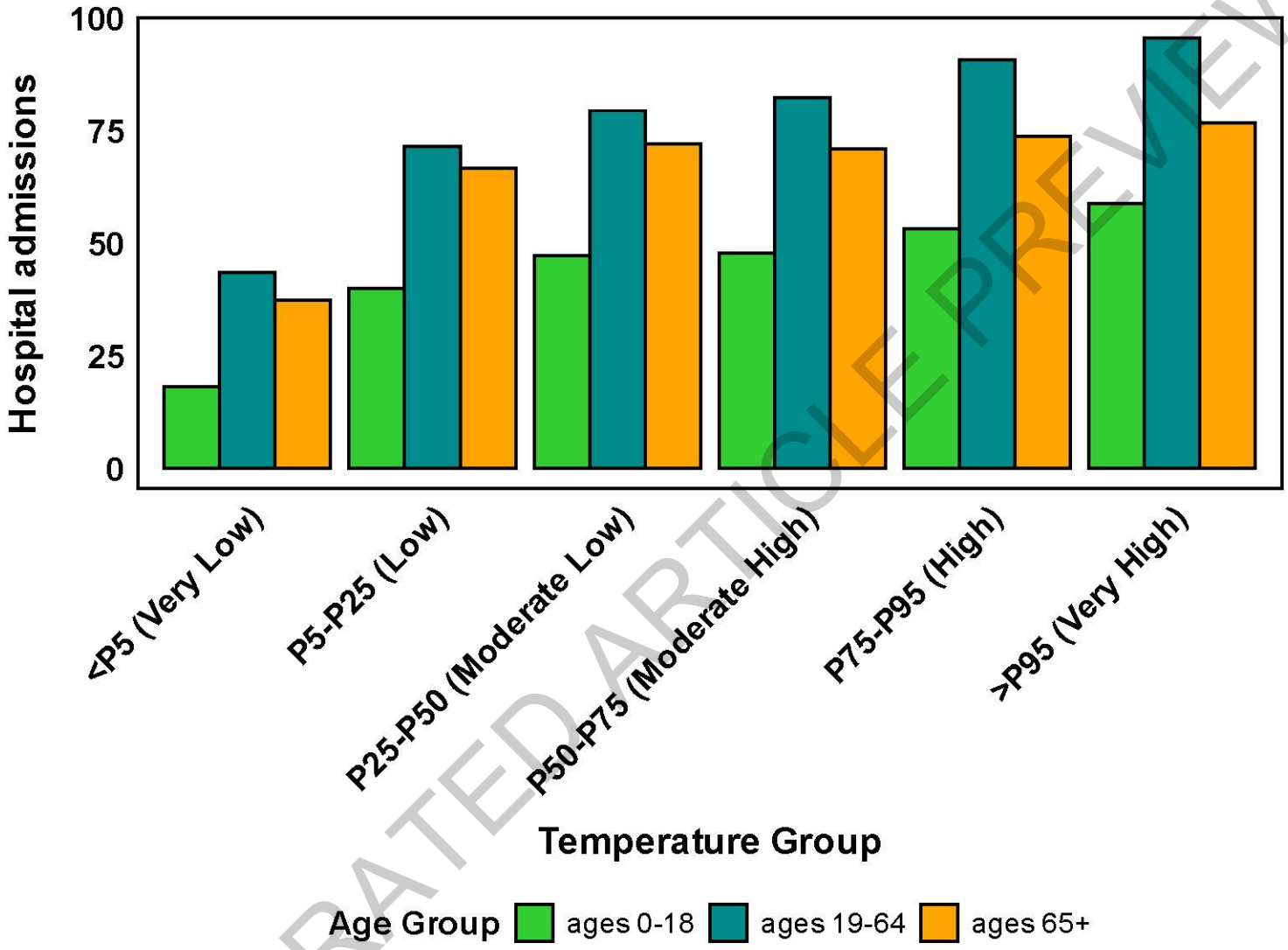

Extended Data Fig. 5

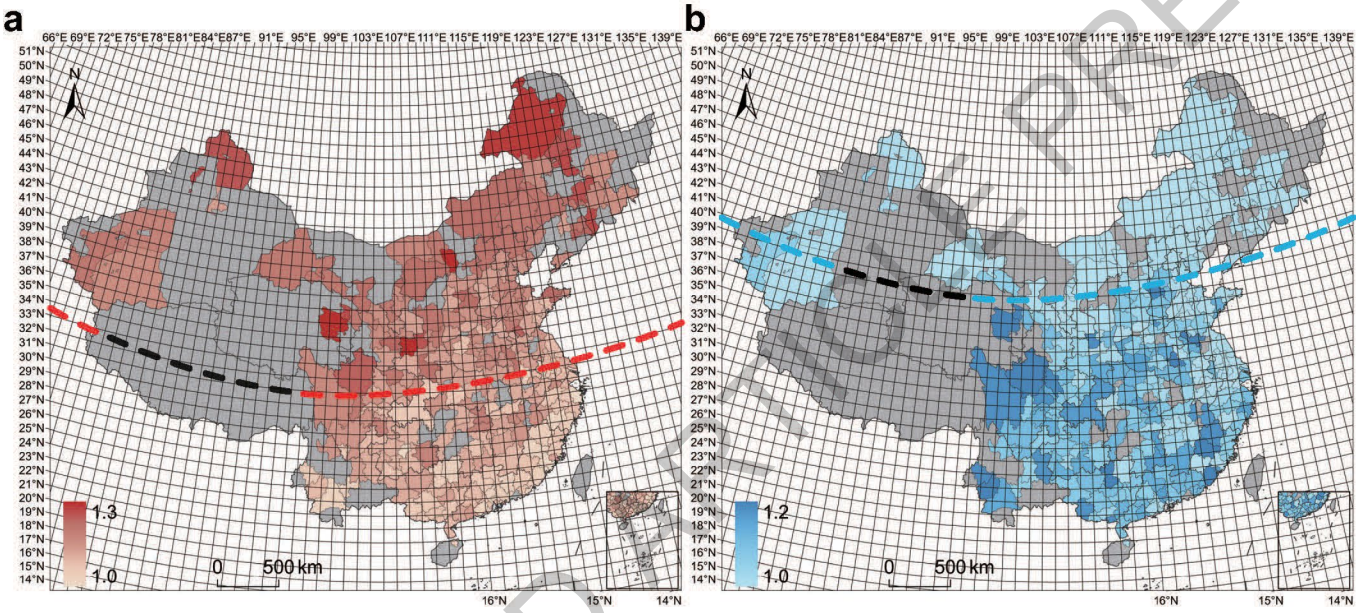

Extended Data Fig. 6

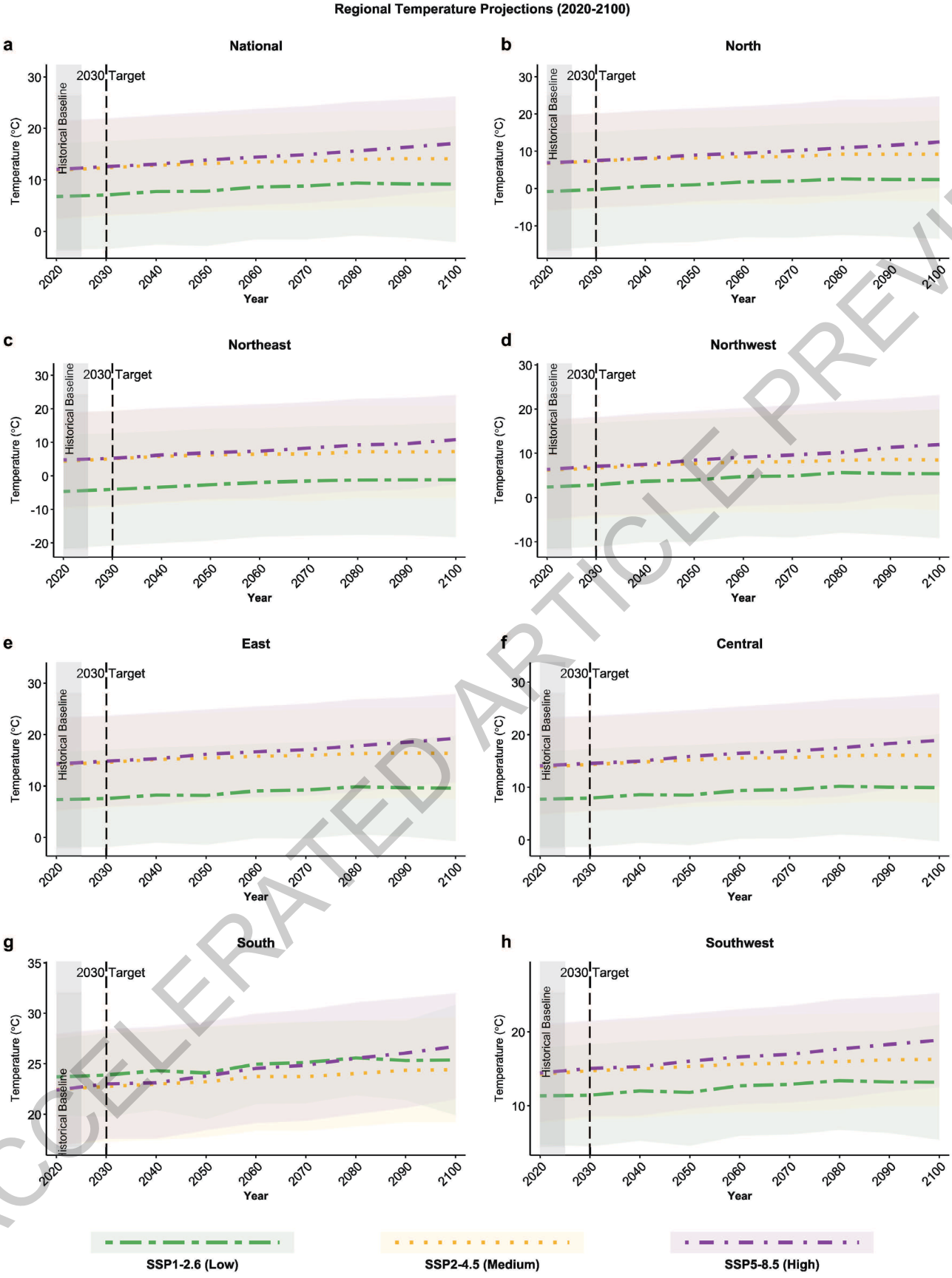

Extended Data Fig. 7

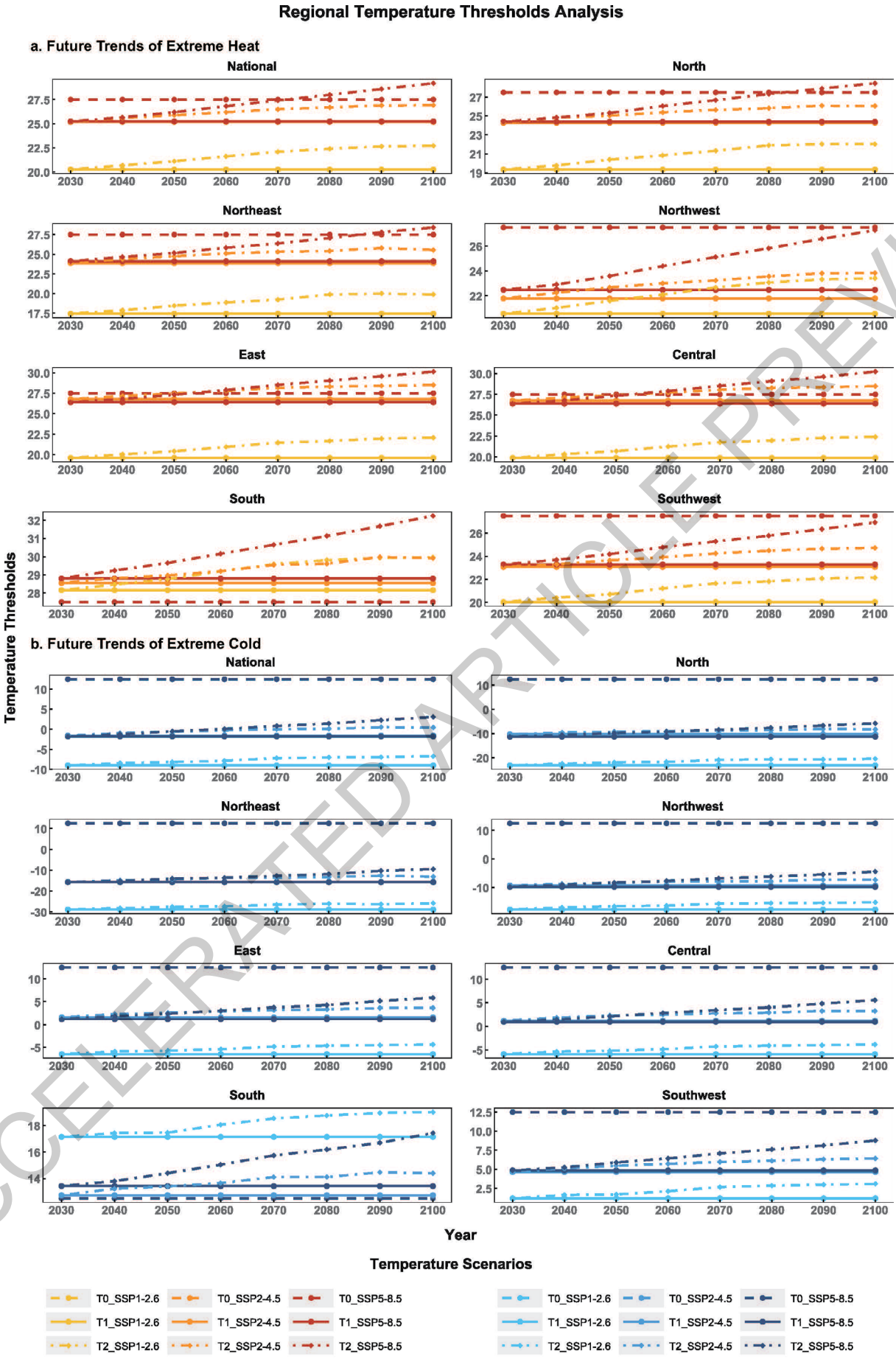

Extended Data Fig. 8

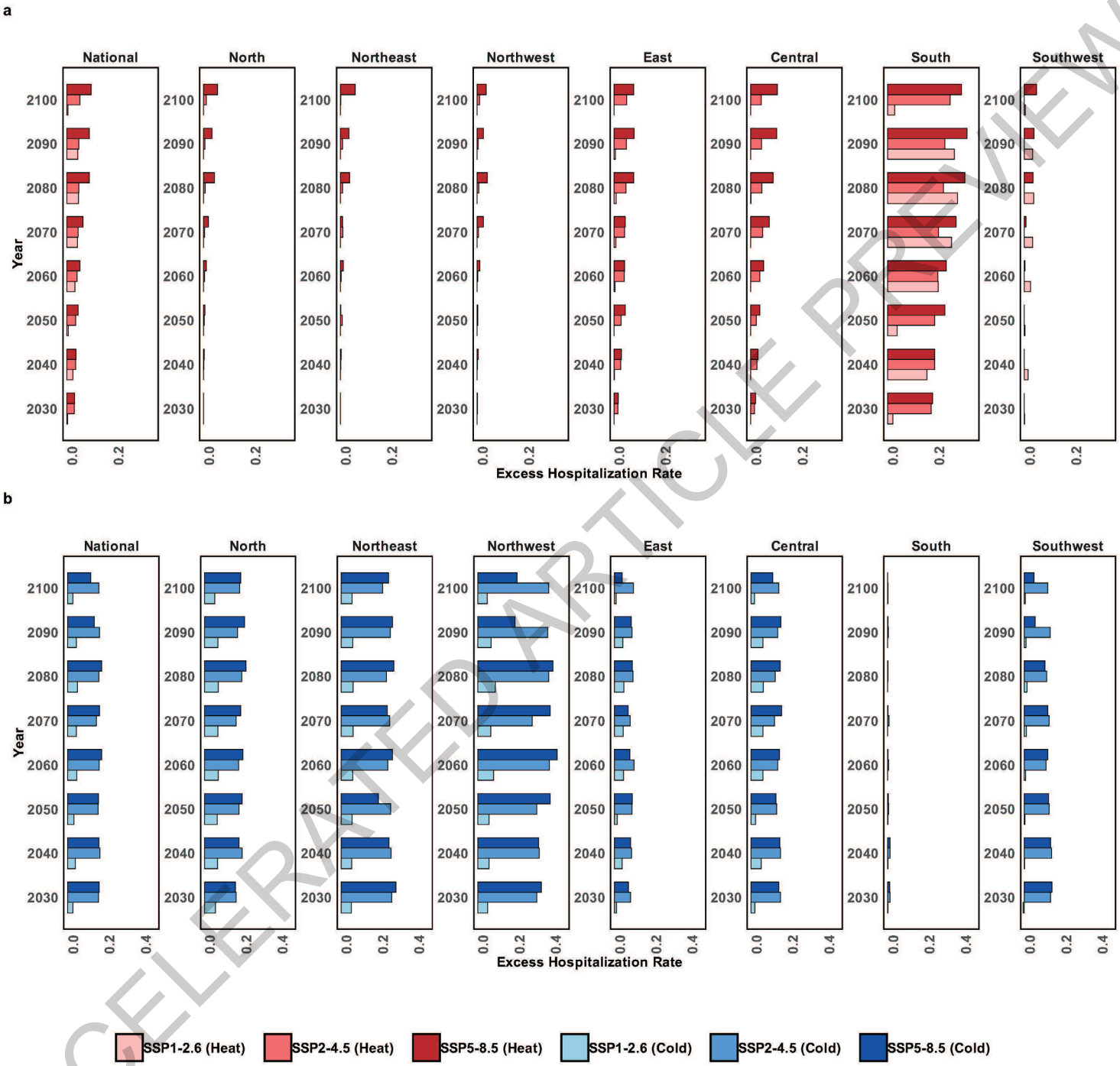

Extended Data Fig. 9

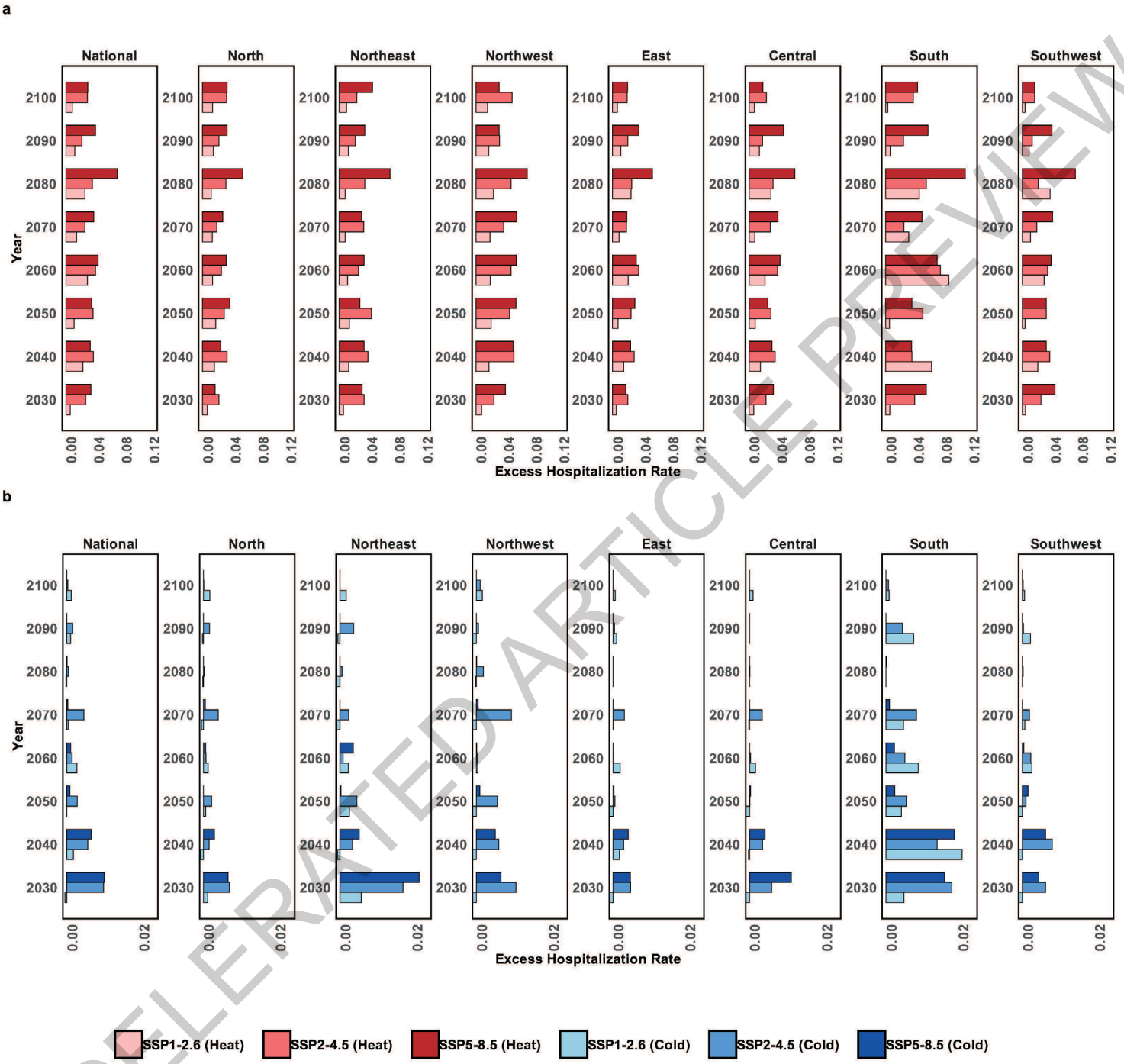

Extended Data Fig. 10

a. Cost by Region and Pathway

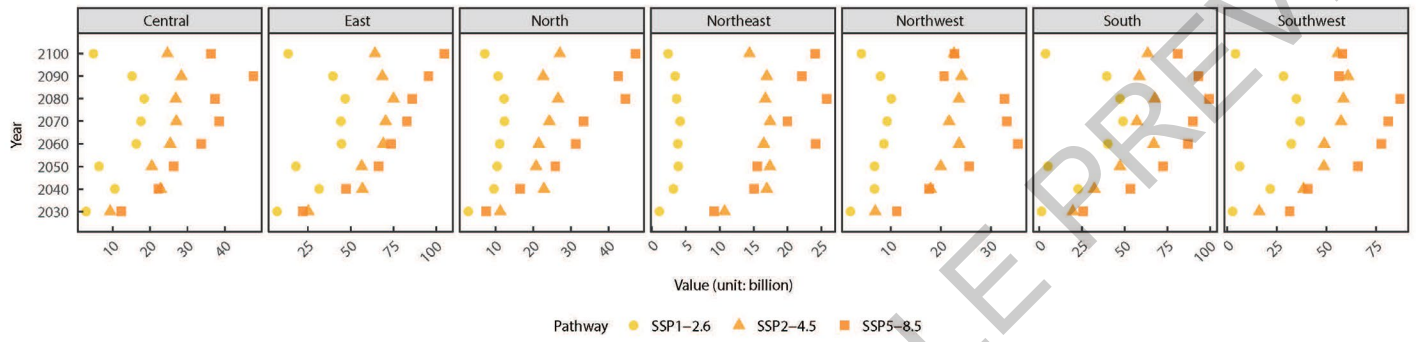

b. GDP by Region and Pathway

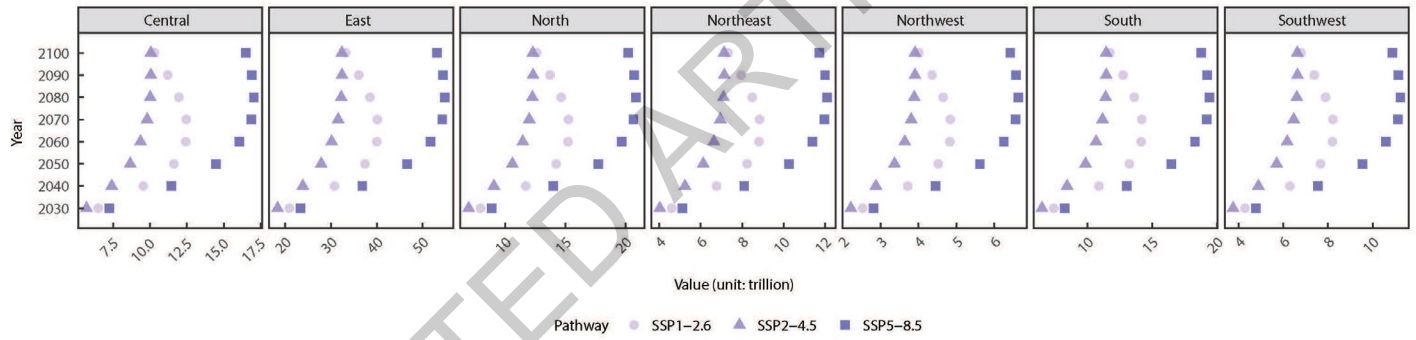

Extended Data Fig. 11

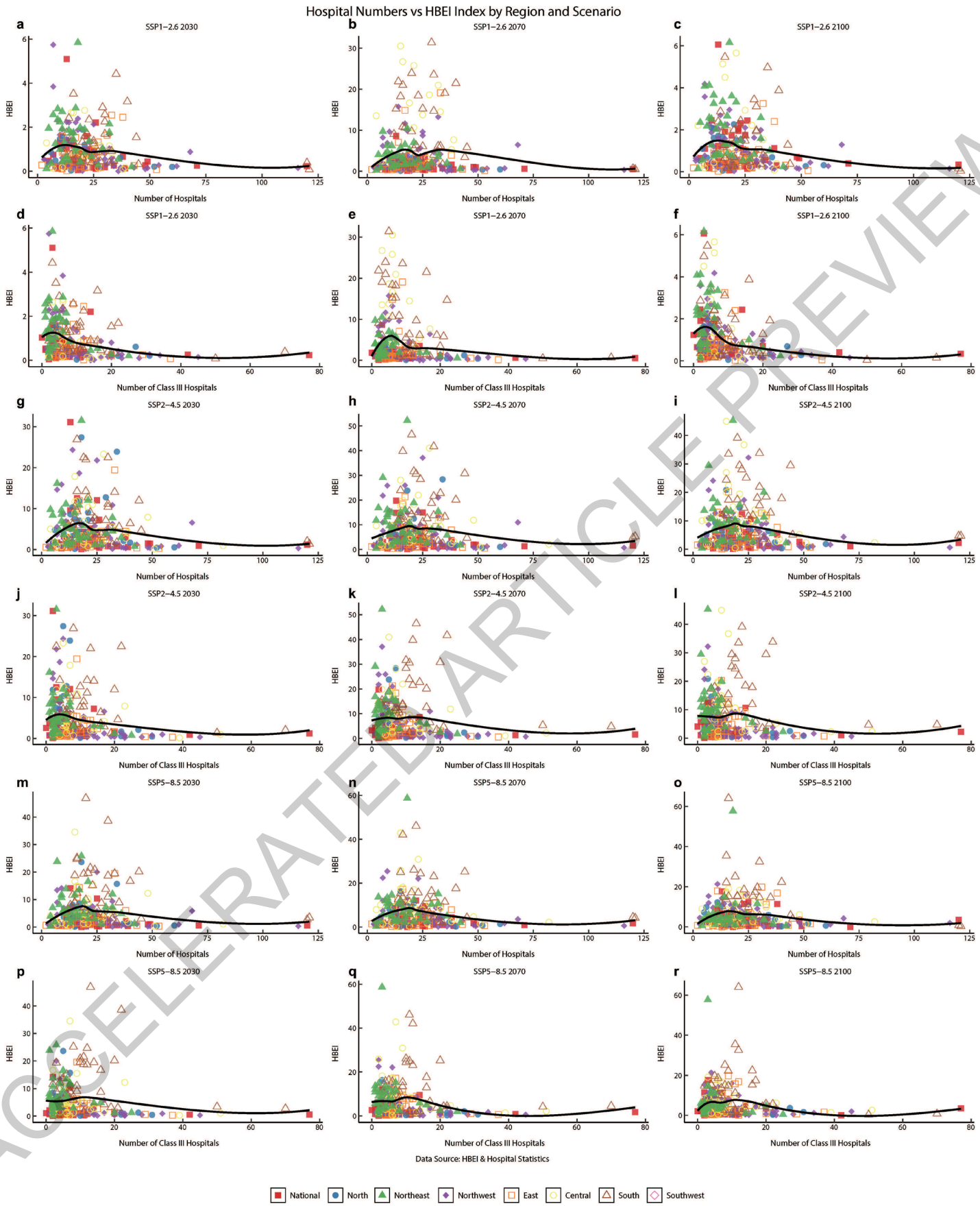

Extended Data Fig. 12

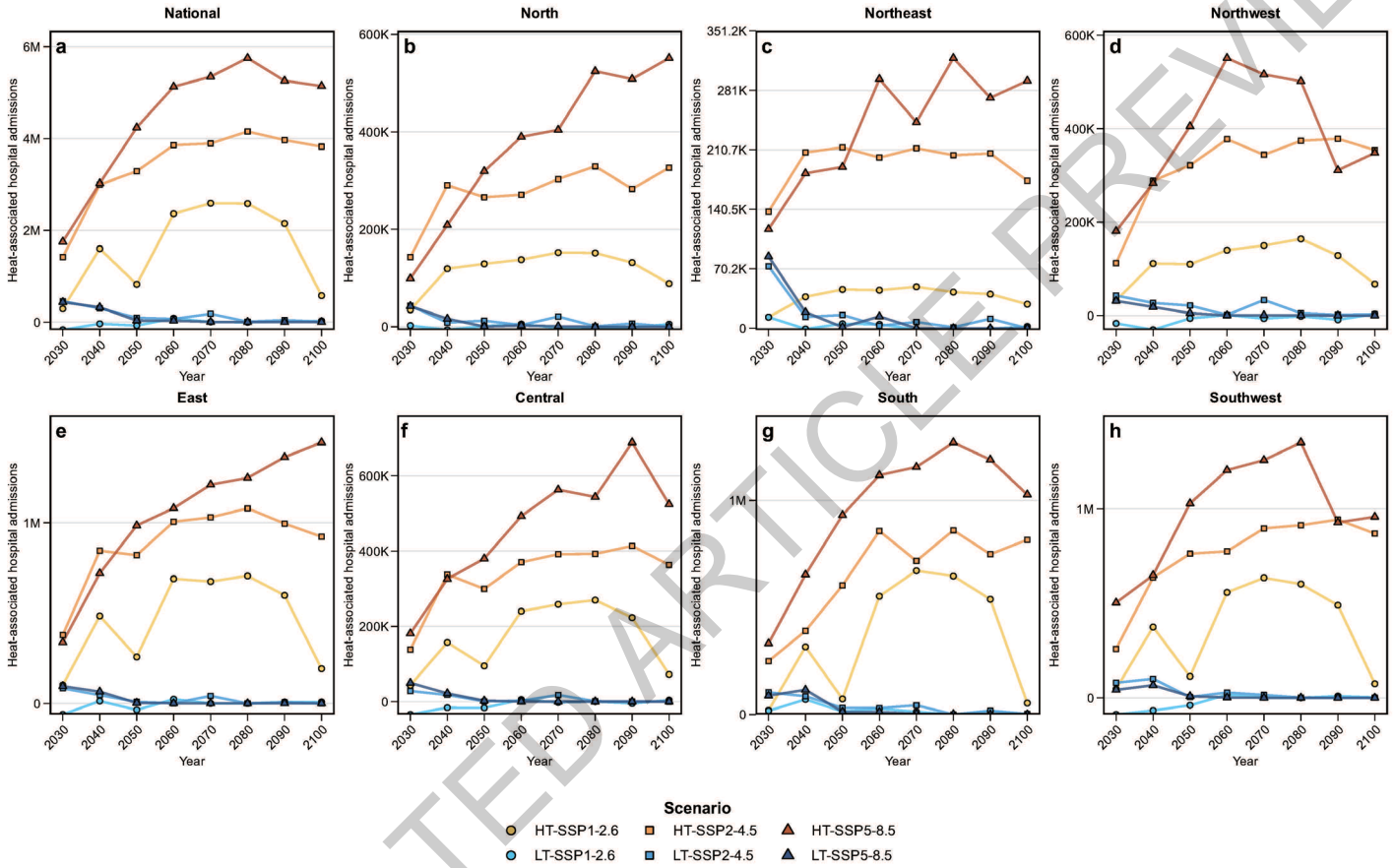

Extended Data Fig. 13

nature portfolio

Corresponding author(s): Wei Pan

Last updated by author(s): Jun 27, 2025

Reporting Summary

Nature Portfolio wishes to improve the reproducibility of the work that we publish. This form provides structure for consistency and transparency in reporting. For further information on Nature Portfolio policies, see our Editorial Policies and the Editorial Policy Checklist.

Statistics

For all statistical analyses, confirm that the following items are present in the figure legend, table legend, main text, or Methods section.

n/a	Confirmed
☐	☒ The exact sample size (*n*) for each experimental group/condition, given as a discrete number and unit of measurement
☐	☒ A statement on whether measurements were taken from distinct samples or whether the same sample was measured repeatedly
☐	☒ The statistical test(s) used AND whether they are one- or two-sided *Only common tests should be described solely by name; describe more complex techniques in the Methods section.*
☐	☒ A description of all covariates tested
☐	☒ A description of any assumptions or corrections, such as tests of normality and adjustment for multiple comparisons
☐	☒ A full description of the statistical parameters including central tendency (e.g. means) or other basic estimates (e.g. regression coefficient) AND variation (e.g. standard deviation) or associated estimates of uncertainty (e.g. confidence intervals)
☐	☒ For null hypothesis testing, the test statistic (e.g. *F*, *t*, *r*) with confidence intervals, effect sizes, degrees of freedom and *P* value noted *Give P values as exact values whenever suitable.*
☒	☐ For Bayesian analysis, information on the choice of priors and Markov chain Monte Carlo settings
☒	☐ For hierarchical and complex designs, identification of the appropriate level for tests and full reporting of outcomes
☒	☐ Estimates of effect sizes (e.g. Cohen's *d*, Pearson's *r*), indicating how they were calculated

Our web collection on statistics for biologists contains articles on many of the points above.

Software and code

Policy information about availability of computer code

Data collection	Data collection was conducted on the Windows 10 operating system. Hospital discharge records were obtained from over 7,000 hospitals across China, with relevant hospitalization indicators and associated costs systematically collected.
Data analysis	The data were preprocessed using Python (version 3.11) to generate model-ready datasets and perform temperature prediction. Subsequently, model estimation and predictive analyses were conducted in R (version 4.3.2). Distributed lag nonlinear models (DLNM) and future predictive analyses were implemented in R using the following packages: dlnm (2.4.7), dplyr (1.1.4), splines (4.3.2), tsModel (0.6-2), mvmeta (1.0.3), lubridate (1.9.3), stringr (1.5.1), readxl (1.4.3), forecast (8.24.0). All of the codes can be accessed at https://zenodo.org/records/15752585

For manuscripts utilizing custom algorithms or software that are central to the research but not yet described in published literature, software must be made available to editors and reviewers. We strongly encourage code deposition in a community repository (e.g. GitHub). See the Nature Portfolio guidelines for submitting code & software for further information.

Data

Policy information about availability of data

All manuscripts must include a data availability statement. This statement should provide the following information, where applicable:

- Accession codes, unique identifiers, or web links for publicly available datasets
- A description of any restrictions on data availability
- For clinical datasets or third party data, please ensure that the statement adheres to our policy

The national hospitalization data are confidential and obtained from the National Health Commission of China. To enhance transparency while adhering to data protection policies, we have publicly released city-level daily hospitalization counts and average hospitalization costs, with all city names anonymized and replaced by coded identifiers. All shared data are accessible via [https://zenodo.org/records/15752585]. Meteorological data were obtained from the ECMWF ERA5 dataset (https://cds.climate.copernicus.eu/cdsapp#!/dataset/sis-agrometeorological-indicators?tab=overview). The temperature data used for forecasting were sourced from the CMIP6 dataset (https://cds.climate.copernicus.eu/datasets/projections-cmip6?tab=overview).The population projection data were derived from publicly available data in a research paper (https://cloud.tsinghua.edu.cn/f/d593f46793fb4145b8b9/?dl=1). The GDP projection data were obtained from publicly available data in a research paper (https://zenodo.org/records/5880037). Other economic and geographic information related to Chinese cities was sourced from the National Bureau of Statistics of China (https://www.stats.gov.cn/sj/ndsj/).

Research involving human participants, their data, or biological material

Policy information about studies with human participants or human data. See also policy information about sex, gender (identity/presentation), and sexual orientation and race, ethnicity and racism.

Reporting on sex and gender	Gender data were derived from self-reports by hospitalized patients. Informed consent was obtained for the collection and sharing of individual-level data. The source dataset included categorized gender information, comprising 33,751,524 males and 27,947,474 females.
Reporting on race, ethnicity, or other socially relevant groupings	No socially constructed variables related to populations (e.g., gender, race, ethnicity, etc.) were used for analysis in this study.
Population characteristics	See above.
Recruitment	Regarding the "Human research participants" option in the Editorial Policy Checklist, we clarify that our study analyzed fully de-identified hospitalization records provided directly by the National Health Commission (NHC) of China. The NHC performed irreversible anonymization prior to data release, removing all personal identifiers and sensitive attributes. Consequently, the dataset contains no traceable individual-level information. We therefore maintain that this policy item is not applicable.
Ethics oversight	This study was approved by Medical Ethics Committee, Zhongnan Hospital of Wuhan University (Approval No. 2024297K, Approval Date: 10, December 2024). All procedures adhered to the ethical standards of this committee and applicable national regulations. The revised manuscript reflects this addition, and the ethics documentation remains available for editorial verification upon request.

Note that full information on the approval of the study protocol must also be provided in the manuscript.

Field-specific reporting

Please select the one below that is the best fit for your research. If you are not sure, read the appropriate sections before making your selection.

☐ Life sciences ☐ Behavioural & social sciences ☒ Ecological, evolutionary & environmental sciences

For a reference copy of the document with all sections, see nature.com/documents/nr-reporting-summary-flat.pdf

Ecological, evolutionary & environmental sciences study design

All studies must disclose on these points even when the disclosure is negative.

Study description	This study aims to assess and project the impacts of extreme temperature events on hospital admission risks and associated medical expenses for residents from 2030 to 2100. The study employs retrospective epidemiological analysis and scenario-based projections, integrating historical meteorological data, population health information, and economic healthcare costs. Simulation analyses are conducted using climate model projections under Representative Concentration Pathways (RCPs), including RCP2.6, RCP4.5, and RCP8.5 scenarios.The research is structured as a two-factor experimental design involving two primary treatment factors: (1) temperature exposure scenarios (extreme heat and extreme cold); and (2) demographic characteristics (age stratification into children, adults, and elderly groups). A hierarchical design structure is employed, nested within distinct geographic regions, to evaluate regional differences and interaction effects of vulnerability characteristics. Experimental units are defined at the city (or county/district) population level, with repeated measurements conducted at multiple time points at decadal intervals throughout the 2030-2100 period.

Research sample	The research sample comprises hospitalization records collected from 301 cities across China, spanning January 1, 2021, to December 31, 2023. The dataset, sourced from the Clinical Pathway Database (CPD) managed by the National Health Commission of China, contains demographic and hospitalization data covering patients of all age groups and both sexes. The CPD aggregates medical records from over 7,000 hospitals nationwide, ensuring extensive geographical and demographic coverage. This comprehensive dataset was selected to represent hospitalization patterns and medical care needs across the general population of China, capturing regional variations in hospital admissions and healthcare utilization related to extreme temperature events. No experimental manipulations were applied, as the study utilizes existing datasets to perform observational analyses and projections.
Sampling strategy	The study utilizes data from the Clinical Pathway Database (CPD), managed by the National Health Commission of China, which aggregates hospitalization records from more than 7,000 hospitals nationwide. The data were collected using a hospital-level random sampling procedure to report treatment details for various disease categories, with sampling ratios ranging from 60% to 100%. Although no formal statistical calculation was conducted to predetermine sample size, the selected sample covers approximately one-third of the average annual hospitalizations in China from 2021 to 2023. This extensive sample size was chosen based on its representativeness and geographical comprehensiveness, ensuring robust statistical power and generalizability of findings across diverse regions and populations within China.
Data collection	The primary data were obtained from standardized hospital discharge records (front-page medical records). These records were completed by physicians from various hospitals during routine clinical practice and subsequently reported to the Clinical Pathway Database (CPD). Specifically, physicians recorded patient demographic information, diagnoses, treatment details, and hospitalization outcomes. These standardized forms were then submitted electronically by each hospital to the CPD, ensuring consistency and accuracy in data aggregation across participating institutions.
Timing and spatial scale	Data collection began on January 1, 2021, and concluded on December 31, 2023, with hospital-level random sampling conducted continuously and reported on an annual basis. The annual sampling frequency was selected to align with standardized hospital reporting cycles, ensuring data consistency and comparability across different years. No gaps occurred within this data collection period. The data encompass a nationwide spatial scale, covering 301 cities across China and reflecting diverse geographic and climatic regions, which ensures robust representativeness for evaluating hospitalizations related to extreme temperature events across the country.
Data exclusions	No data were excluded from the analyses.
Reproducibility	As this study is based on observational data rather than experimental interventions, reproducibility was assessed through data validation and robustness checks. Sensitivity analyses were conducted to verify the consistency of findings across different temperature exposure scenarios, demographic subgroups, and geographic regions. Additionally, hospitalization trends were cross-validated against independent national health statistics to ensure consistency. All analytical procedures were repeated using different statistical models to confirm the robustness of the results, and no attempts to replicate the analyses failed.
Randomization	Since this study is based on observational hospitalization data rather than experimental interventions, no random allocation into groups was performed. Instead, participants were categorized based on naturally occurring variables, including temperature exposure scenarios (extreme heat and extreme cold), demographic characteristics (age groups: children, adults, elderly), and temperature-sensitive diseases (respiratory, circulatory, urinary, endocrine, and neurological conditions). To control for potential confounders, statistical adjustments were applied, including covariate adjustments for demographic factors, pre-existing health conditions, and regional socioeconomic differences. Analytical methods such as stratification and multivariable regression models were employed to mitigate bias and isolate the impact of extreme temperatures on hospitalization outcomes.
Blinding	Blinding was not applicable to this study, as it is based on observational hospitalization data rather than experimental interventions. The data were collected through routine hospital reporting systems, where physicians recorded patient information during clinical care without knowledge of the study objectives. Additionally, data analysis was conducted using anonymized records, ensuring that researchers had no access to personally identifiable information, thus minimizing potential bias in data interpretation.

Did the study involve field work? ☐ Yes ☒ No

Reporting for specific materials, systems and methods

We require information from authors about some types of materials, experimental systems and methods used in many studies. Here, indicate whether each material, system or method listed is relevant to your study. If you are not sure if a list item applies to your research, read the appropriate section before selecting a response.

Materials & experimental systems

n/a	Involved in the study
☒	☐ Antibodies
☒	☐ Eukaryotic cell lines
☒	☐ Palaeontology and archaeology
☒	☐ Animals and other organisms
☒	☐ Clinical data
☒	☐ Dual use research of concern
☒	☐ Plants

Methods

n/a	Involved in the study
☒	☐ ChIP-seq
☒	☐ Flow cytometry
☒	☐ MRI-based neuroimaging

Plants

Seed stocks	*Report on the source of all seed stocks or other plant material used. If applicable, state the seed stock centre and catalogue number. If plant specimens were collected from the field, describe the collection location, date and sampling procedures.*
Novel plant genotypes	*Describe the methods by which all novel plant genotypes were produced. This includes those generated by transgenic approaches, gene editing, chemical/radiation-based mutagenesis and hybridization. For transgenic lines, describe the transformation method, the number of independent lines analyzed and the generation upon which experiments were performed. For gene-edited lines, describe the editor used, the endogenous sequence targeted for editing, the targeting guide RNA sequence (if applicable) and how the editor was applied.*
Authentication	*Describe any authentication procedures for each seed stock used or novel genotype generated. Describe any experiments used to assess the effect of a mutation and, where applicable, how potential secondary effects (e.g. second site T-DNA insertions, mosiacism, off-target gene editing) were examined.*